

**STRUCTURAL DISORDER WITHIN  
FLUORITE STRUCTURED  
SUPERIONIC CONDUCTORS.**

**Steve Hull.**

**The ISIS Facility,  
Rutherford Appleton Laboratory,  
U.K.**



# ACKNOWLEDGEMENTS

Ray Osborn (Argonne)

Jon Goff (Liverpool)

Bill Hayes (Oxford)

Michael Hofmann (Munich)

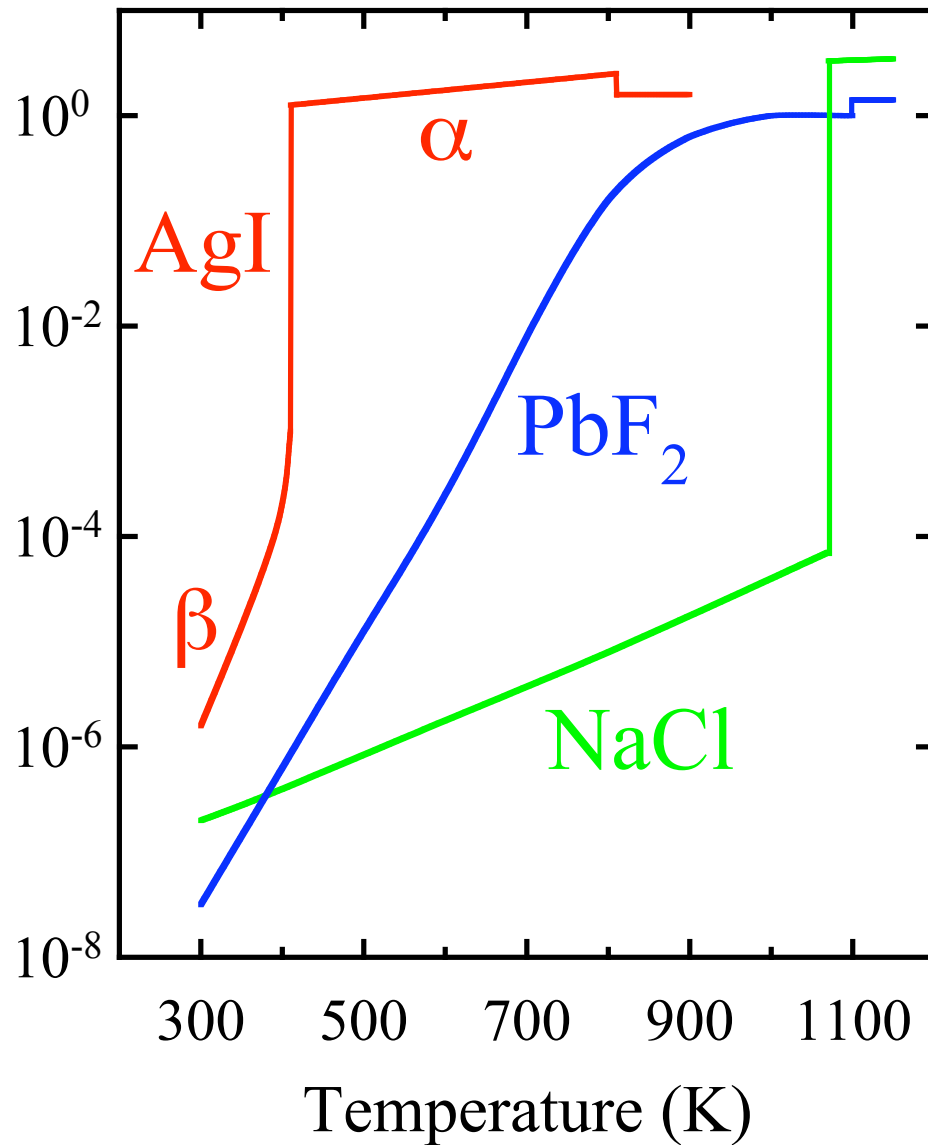
Mike Hutchings (Harwell)

Dave Keen (Oxford / ISIS)

Chick Wilson (ISIS)

Funded by UK Engineering and Physical Sciences  
Research Council

# INTRODUCTION TO SUPERIONIC CONDUCTORS



‘Normal’ ionic conductor **NaCl** has a finite ionic conductivity due to the presence of thermally induced lattice defects.

Superionic conductors possess exceptionally high values of their ionic conductivity ( $\sim 10^0 \text{ S cm}^{-1}$ ) whilst in the solid state.

Type-I Superionics :  
**AgI**, CuI,  $\text{Ag}_2\text{Te}$ , *etc.*

Type-II Superionics :  
 **$\text{PbF}_2$** ,  $\text{CaF}_2$ ,  $\text{UO}_2$ , *etc.*

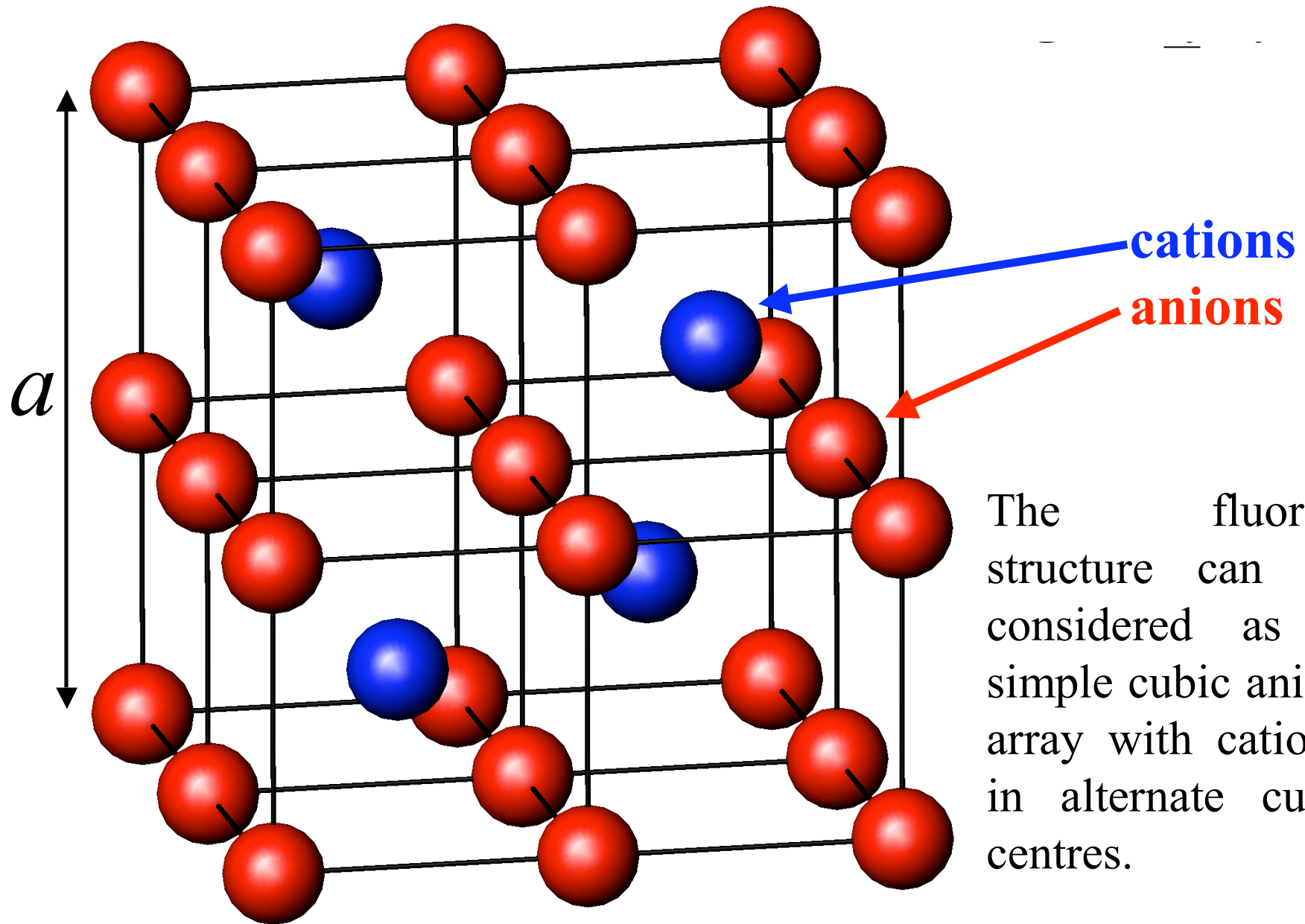
# SUMMARY OF RESEARCH PROGRAMME

- Structural properties of superionic compounds.
  - Principally using neutron diffraction.
  - Bragg scattering  $\square$  time-averaged structure.
  - Diffuse scattering  $\square$  short-range correlations.
  - Complementary X-ray diffraction, MD, *etc.*
- What factors influence superionic behaviour?
  - Role of structure, ionic size, polarizability, *etc.*
  - Effect of chemical dopants.
  - High pressure / high temperature studies.
  - Require the use of powder samples.

# OUTLINE OF TALK

- Introduction to Superionic Conductors.
- The Fluorite Crystal Structure.
- Diffuse Scattering Studies of Fluorites.
- Frenkel Defects in Superionic Fluorites.
- Chemical Doping to Reduce  $T_c$ .
- Anion-Excess Fluorite :  $\text{CaF}_2\text{-YF}_3$ .
- Anion-Deficient Fluorite :  $\text{ZrO}_2\text{-Y}_2\text{O}_3$ .
- Bragg and Diffuse Neutron Scattering.
- Quasielastic Neutron Scattering.
- Conclusions.

# THE FLUORITE STRUCTURE



The fluorite structure can be considered as a simple cubic anion array with cations in alternate cube centres.

# THE SUPERIONIC TRANSITION IN FLUORITES

The superionic transition within the fluorite structured compounds is characterised by a rapid, but continuous, increase in  $\sigma$  with temperature and an anomalous peak in the specific heat  $C_p$

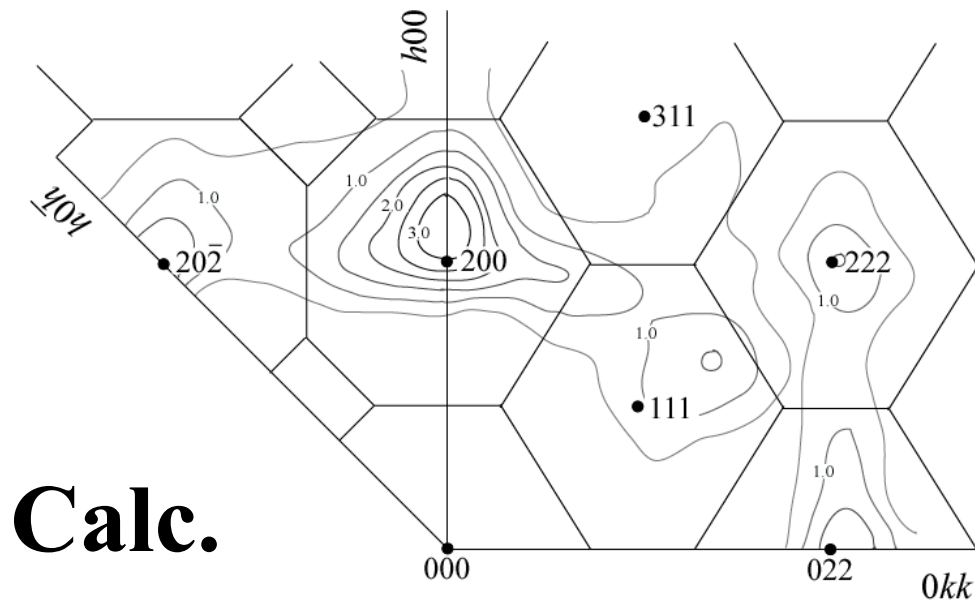
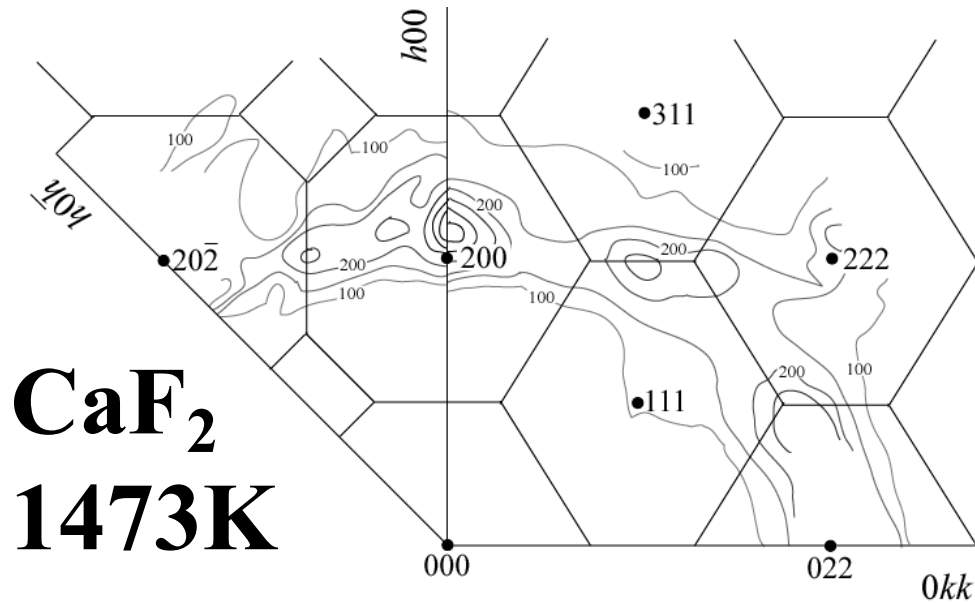


Compound	$T_c$ (K)	$T_c/T_m$
CaF <sub>2</sub>	1430	0.88
SrF <sub>2</sub>	1400	0.81
BaF <sub>2</sub>	1275	0.82
SrCl <sub>2</sub>	1000	0.87
$\square$ -PbF <sub>2</sub>	712	0.61
UO <sub>2</sub>	2610	0.84
ThO <sub>2</sub>	~2950	~0.81

(Schröter and Nolting, 1980)

$\square$ -PbF<sub>2</sub> has lowest  $T_c$  and  $T_c/T_m$  - attributed to higher polarizability of Pb<sup>2+</sup> (Castiglione *et al*, 1999)

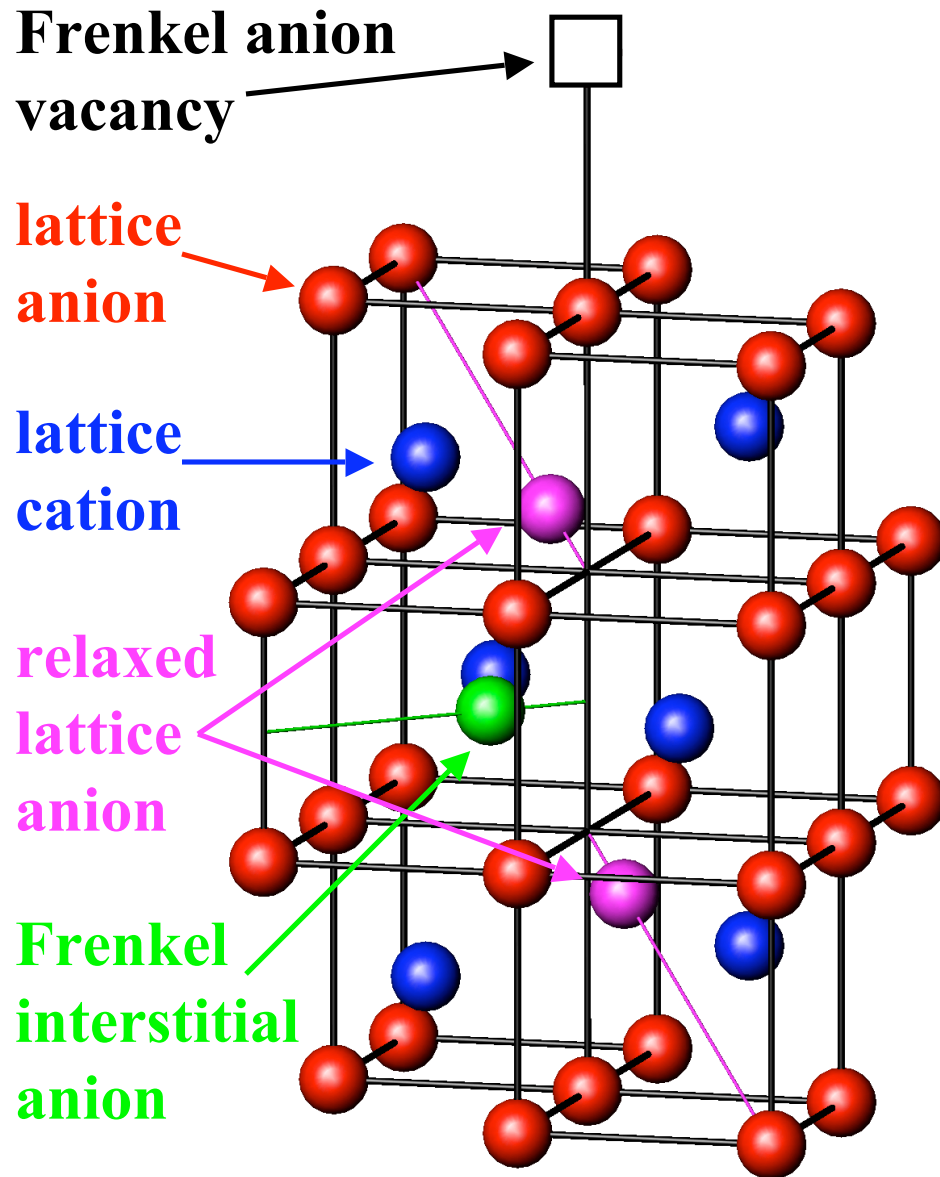
# DIFFUSE NEUTRON SCATTERING



Analysis of Bragg diffraction data collected at  $T > T_c$  showed that a significant fraction of the anions leave the fluorite lattice sites and occupy interstitial positions.

Measurements of the coherent diffuse scattering (using triple-axis spectrometers) showed a characteristic distribution of intensity over reciprocal space which was modelled assuming a distribution of dynamic Frenkel defects (Hutchings *et al.*, 1984).

# FRENKEL DEFECTS IN FLUORITES



The interstitial anion is located between the cube edge and an empty cube centre and causes outward  $\langle 111 \rangle$  relaxations of two nearest neighbour anions.

The diffuse scattering is quasi-elastic  $\square$  lifetime  $\sim 10^{12}$ sec.

Stability of clusters confirmed by static energy calculations (Catlow and Hayes, 1982), but

$n \sim 30-50\%$  - neutrons

$n \sim 2\%$  - MD (Walker, 1982)

Recent work by Madden *et al* (submitted) has resolved this.

# DATA ANALYSIS PROCEDURE

- Extract Bragg intensities from data and perform least-squares refinements to give average structure (positions, occupancies, thermal parameters, *etc.*).
- Devise models of the defect structure (intuition, structures of related compounds, static energy calculations, MD, *etc.*).
- Check that these are consistent with analysis of Bragg diffraction data and any other experimental studies (EXAFS, *etc.*) and have sensible bond lengths, *etc.*
- Calculate the diffuse scattering for all candidate defect clusters and reject those that do not agree well with measured data.
- Perform least-squares fit to diffuse scattering data and select best model. Check that analysis of Bragg and diffuse results agree!
- Perform simultaneous least-squares fit to both datasets to obtain ‘best’ values for positional parameters, thermal parameters, *etc.*

## **ANION-EXCESS FLUORITE : $\text{CaF}_2\text{-YF}_3$**

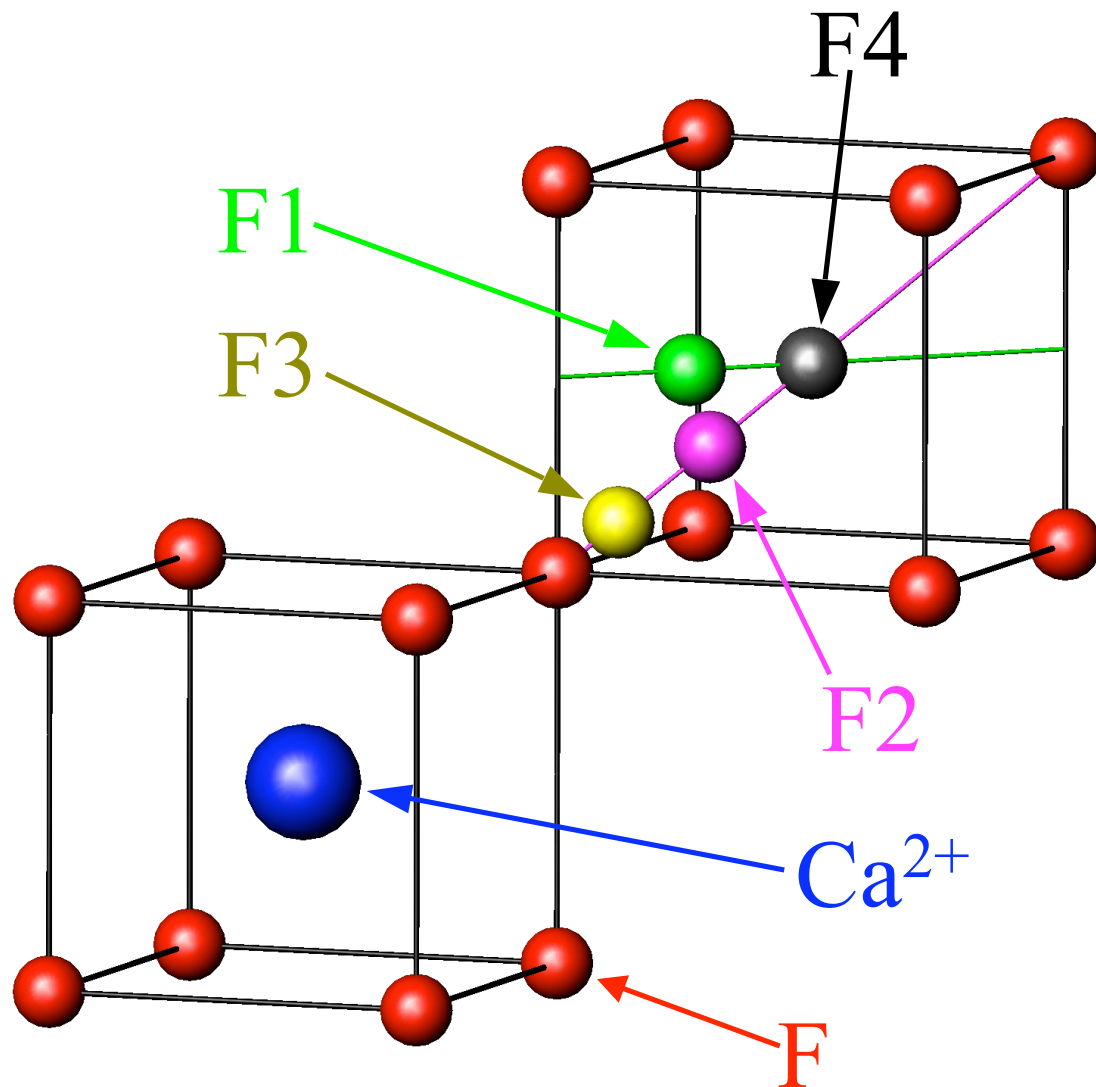
The superionic transition  $T_c$  can be significantly reduced by the addition of aliovalent dopant cations.

For example, the addition of 6%  $\text{YF}_3$  to  $\text{CaF}_2$  causes  $T_c$  to fall from 1430K to  $\sim 1200\text{K}$  (Catlow et al, 1981).

The trivalent dopants are incorporated as substitutional defects on the cation sites and charge neutrality is achieved by incorporating excess anions within interstitial positions.

The manner in which these excess anions are accommodated within the fluorite lattice was studied using a sample of  $(\text{CaF}_2)_{1-x}\text{-(YF}_3)_x$  with  $x=0.06$  and neutron diffraction on SXD at ISIS. High temperature data were collected on IN10 at ILL to investigate the relationship between the extrinsic (chemically induced) and intrinsic (thermally induced) defects.

# CaF<sub>2</sub>-YF<sub>3</sub> : PROPOSED SITES



Diffraction studies of numerous anion-excess fluorites have suggested several different sites for fluorine ions in CaF<sub>2</sub>-YF<sub>3</sub>.

F1 in 48(*i*) at  $\frac{1}{2}, u, u$ , etc.  
with  $u \sim 0.38$

F2 in 32(*f*) at  $w, w, w$ , etc.  
with  $w \sim 0.40$

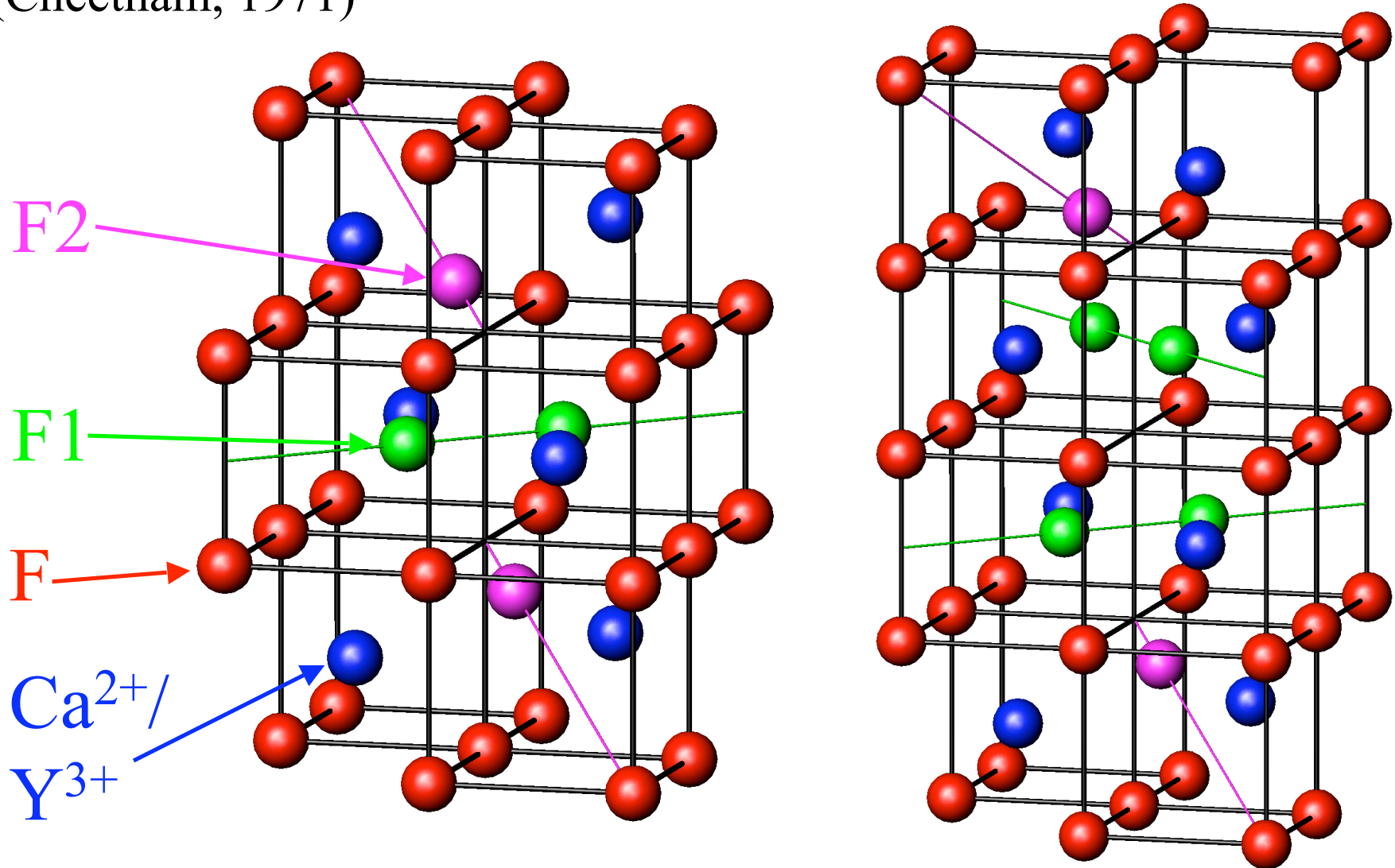
F3 in 32(*f*) at  $v, v, v$ , etc.  
with  $v \sim 0.28$

F4 in 4(*b*) at  $\frac{1}{2}, \frac{1}{2}, \frac{1}{2}$ , etc.

Analysis of Bragg data □  
F1 and F3 occupied

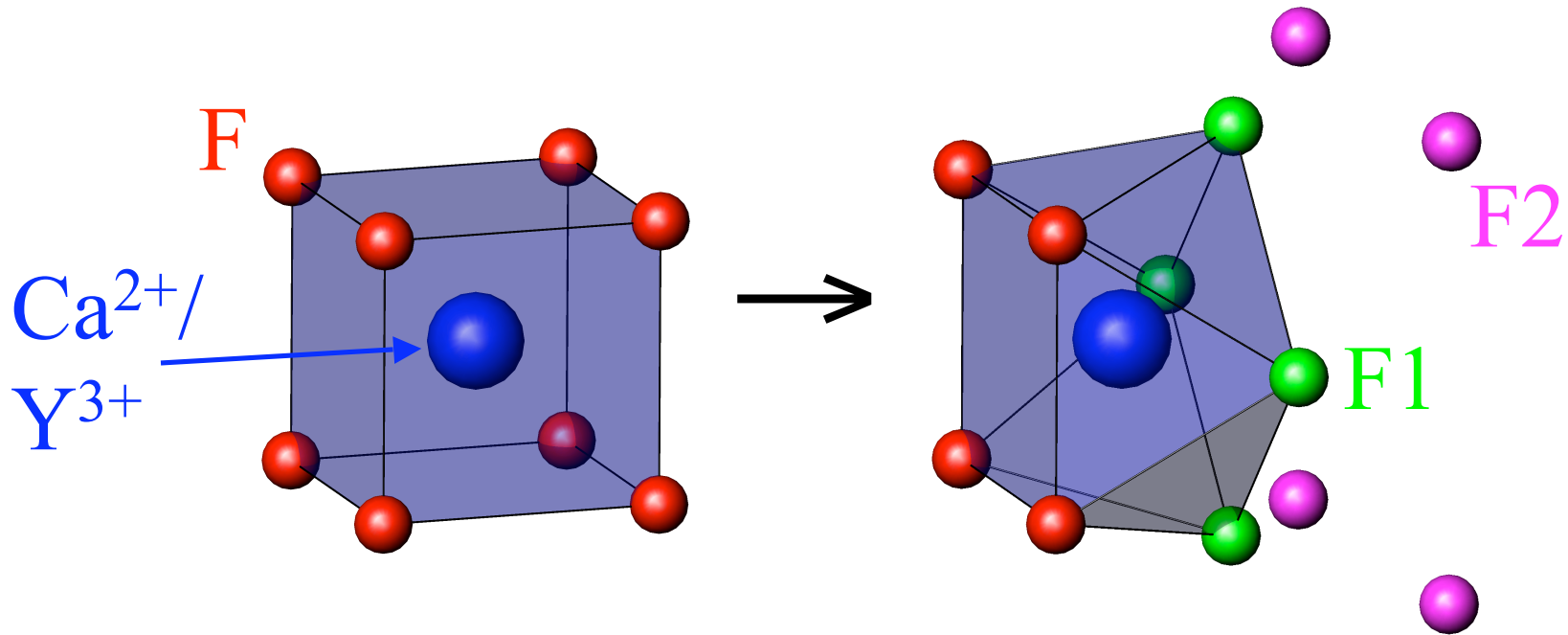
# CaF<sub>2</sub>-YF<sub>3</sub> : DEFECT CLUSTERS

Proposed defect clusters include static versions of Frenkel model.....  
(Cheetham, 1971)



# CaF<sub>2</sub>-YF<sub>3</sub> : DEFECT CLUSTERS

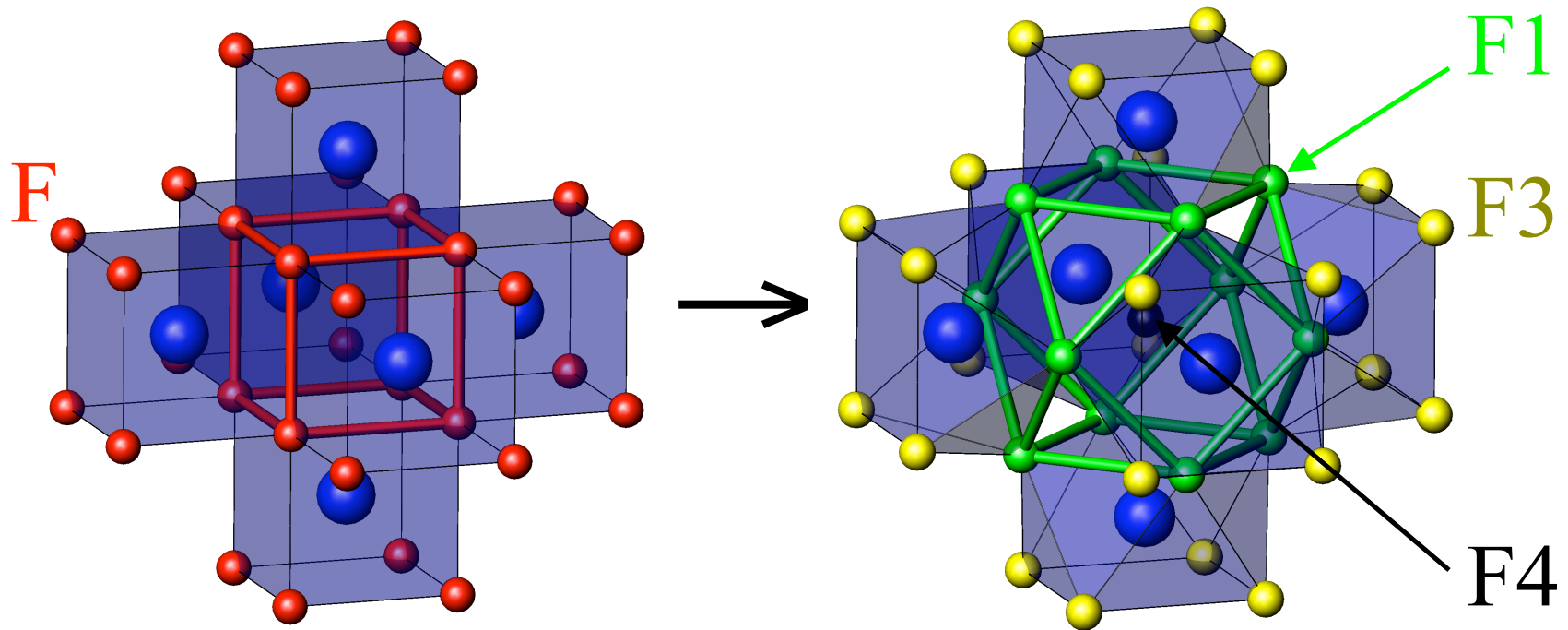
Alternative approach is to convert a CaF<sub>8</sub> cube into a square antiprism by rotating one face by 45° (Laval and Frit, 1983).



This conversion does not incorporate any additional anions into the fluorite lattice. However, it generates sufficient 'empty' space that between one and four anions can be accommodated adjacent to the antiprism (in F2 sites).

## CaF<sub>2</sub>-YF<sub>3</sub> : DEFECT CLUSTERS

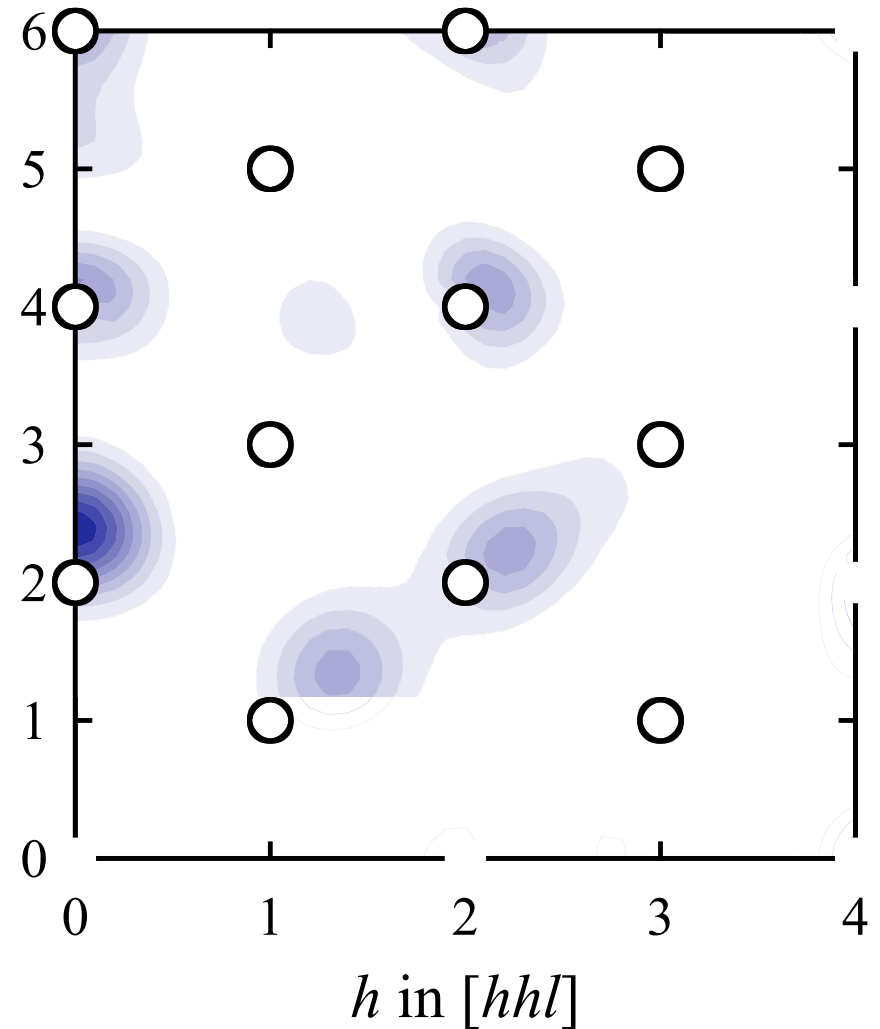
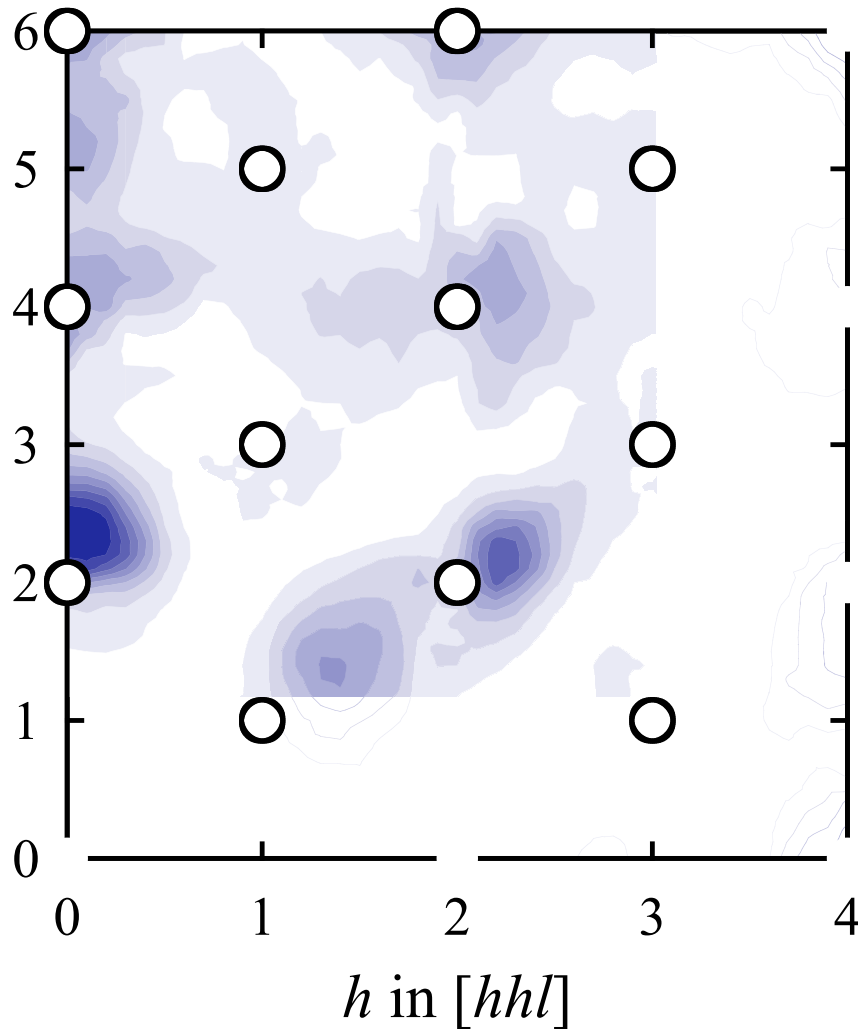
A more complex cluster model involves the simultaneous conversion of six edge-sharing CaF<sub>8</sub> cubes into corner-sharing square antiprisms (Bevan *et al*, 1982)



These ‘cubocathedral’ clusters incorporate four additional anions in F1 sites (or five if the central F4 cavity is also filled). Small outward relaxations of outer anions into F3 sites. There are no F2 anions.

# CaF<sub>2</sub>-YF<sub>3</sub> : DIFFUSE SCATTERING

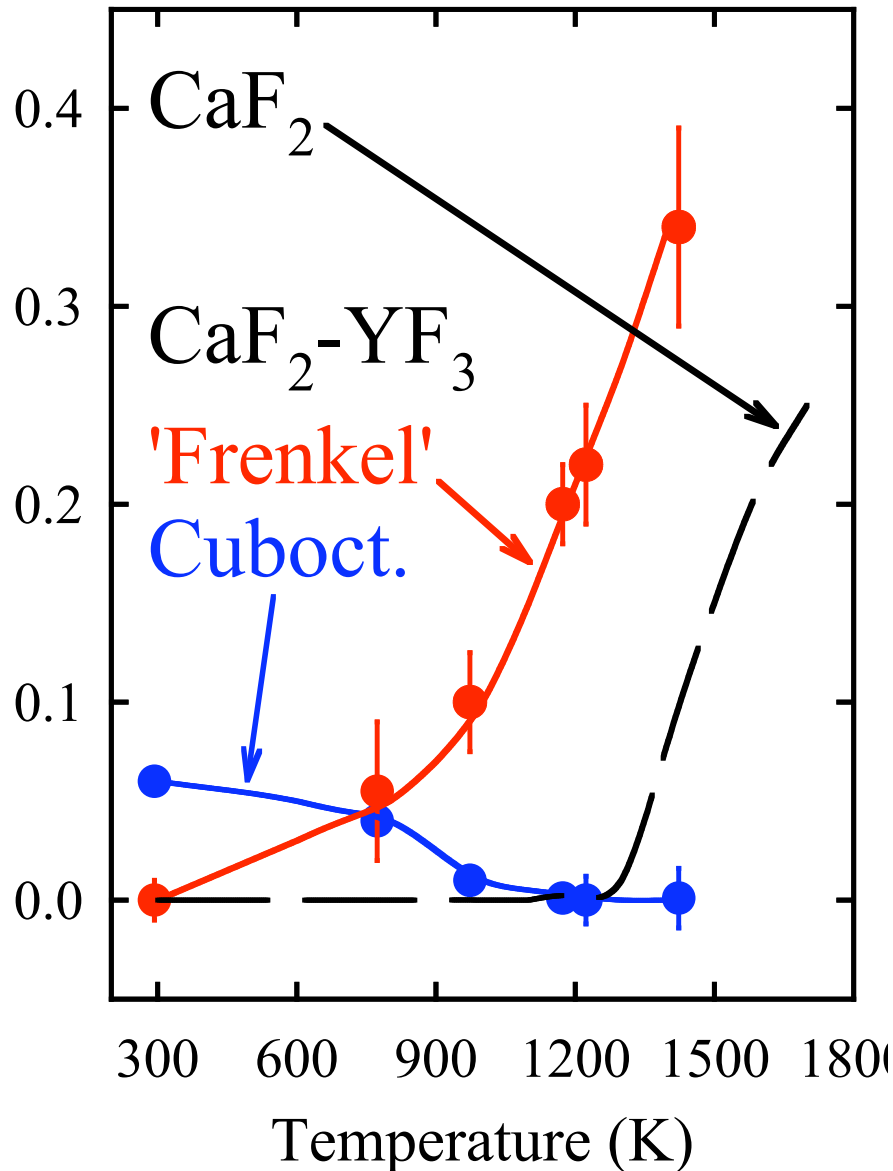
The presence of cuboctahedral clusters within CaF<sub>2</sub>-YF<sub>3</sub> is confirmed by calculation (and fitting) of the diffuse (and Bragg) scattering.



# CaF<sub>2</sub>-YF<sub>3</sub> : BRAGG AND DIFFUSE RESULTS

Ion	Site	Position	Bragg (meas)	Cuboctahedron (calc)	Diffuse (meas)
Ca/Y	4(a)	0,0,0	$B_{\text{iso}}=0.64(1)\text{\AA}^2$		
F	8(c)	$1/4, 1/4, 1/4$	n=1.59(9) $B_{11}=0.60(7)\text{\AA}^2$ $B_{33}=0.81(9)\text{\AA}^2$	n=1.616	
F1	48(i)	$1/2, u, u$	$u=0.390(5)$ n=0.16(2) $B_{\text{iso}}=1.4(4)\text{\AA}^2$	$u=0.354$ n=0.144	$u=0.384(3)$  $B_{\text{iso}}=1.86(8)\text{\AA}^2$
F2	32(f)	w,w,w	$w=0.38(3)$ n=0.01(2) $B_{\text{iso}}=2.2(43)\text{\AA}^2$	n=0.0	
F3	32(f)	v,v,v	$v=0.270(8)$ n=0.31(5) $B_{\text{iso}}=1.1(2)\text{\AA}^2$	$v=0.25$ n=0.288	$v=0.265(5)$  $B_{\text{iso}}=1.21(5)\text{\AA}^2$
F4	4(b)	$1/2, 1/2, 1/2$	n=0.01(3) $B_{\text{iso}}=3.2(55)\text{\AA}^2$	n=0.012	$B_{\text{iso}}=4.6(33)\text{\AA}^2$

## CaF<sub>2</sub>-YF<sub>3</sub> : HIGH TEMPERATURE

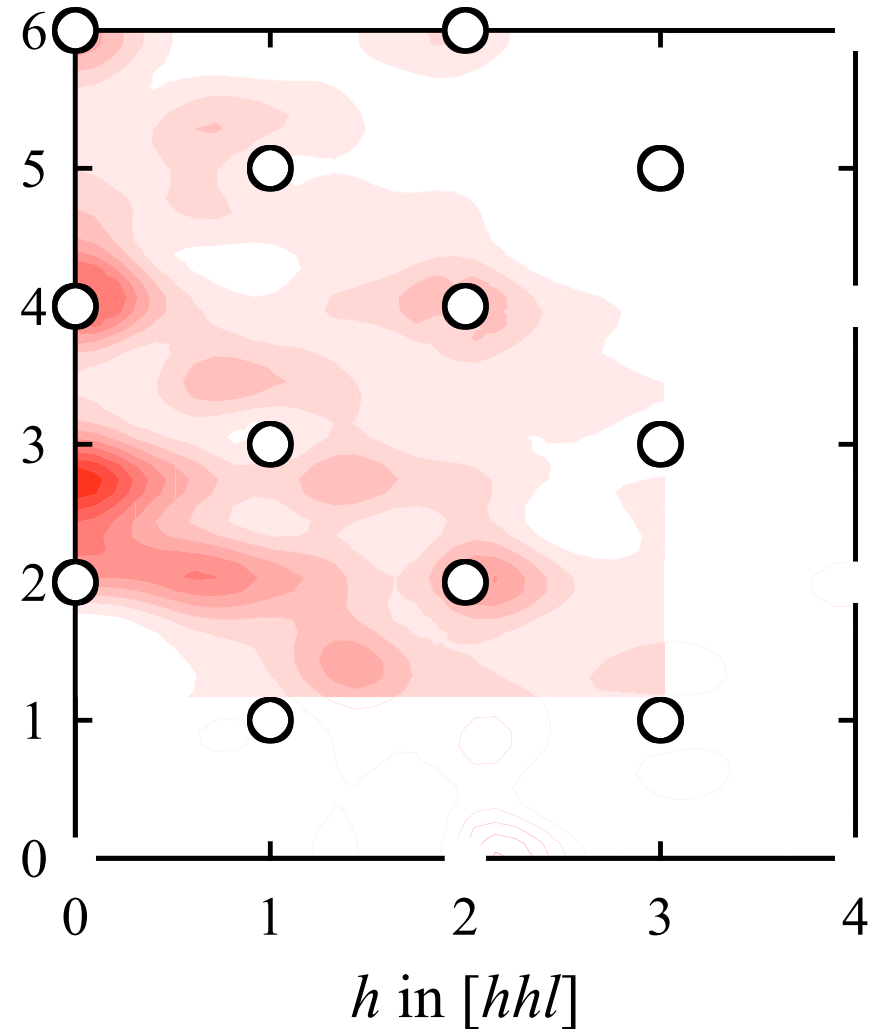
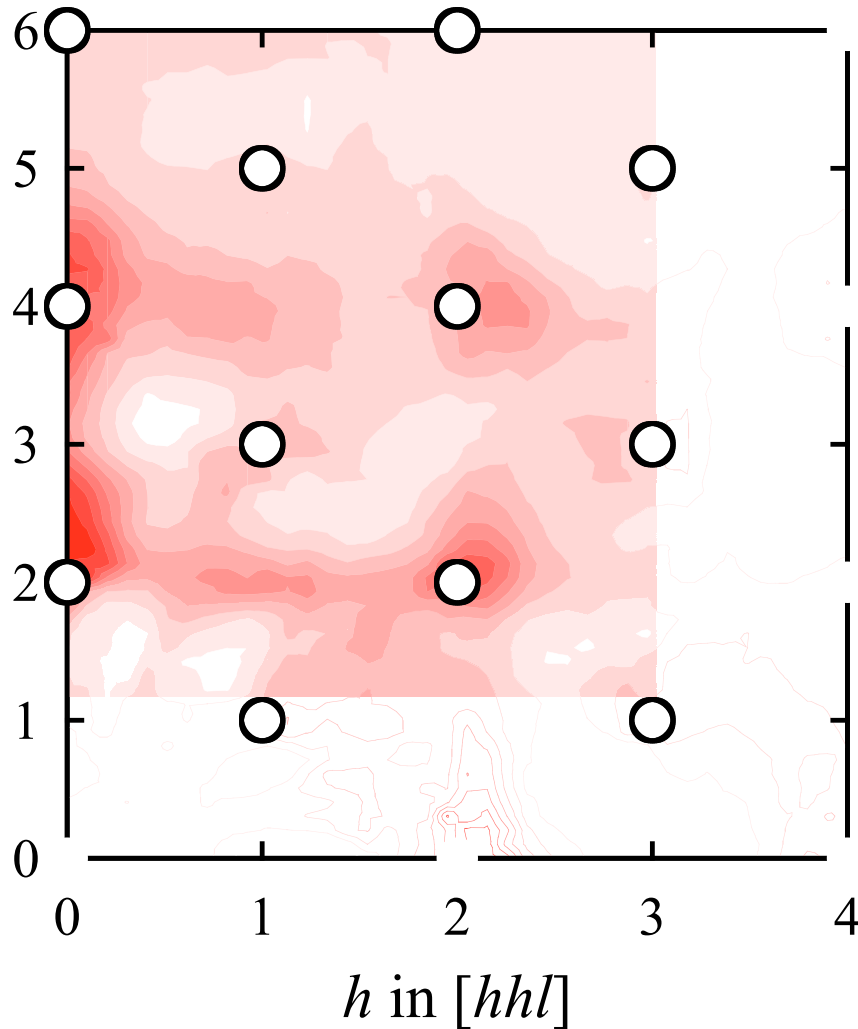


The occupancies of the F1 and F2 sites change on increasing temperature, indicating that the cuboctahedral units break up to form defect clusters similar to the Frenkel defects observed in the undoped fluorites at  $T > T_c$ .

The presence of both extrinsic (chemically induced) and intrinsic (thermally induced) defects within CaF<sub>2</sub>-YF<sub>3</sub> offers an explanation of the higher ionic conductivity of the doped material and is confirmed by diffuse scattering analysis.

# CaF<sub>2</sub>-YF<sub>3</sub> : DIFFUSE SCATTERING

Simultaneous fitting of both Bragg and diffuse scattering components is particularly important for high temperature data (T=1173K).



## ANION-DEFICIENT FLUORITE : $\text{ZrO}_2\text{-Y}_2\text{O}_3$

At room temperature  $\text{ZrO}_2$  has the monoclinic baddelyite structure ( $m\text{-ZrO}_2$ ,  $P2_1/c$ ) with a distorted 7-fold co-ordination of  $\text{O}^{2-}$  around  $\text{Zr}^{4+}$ .

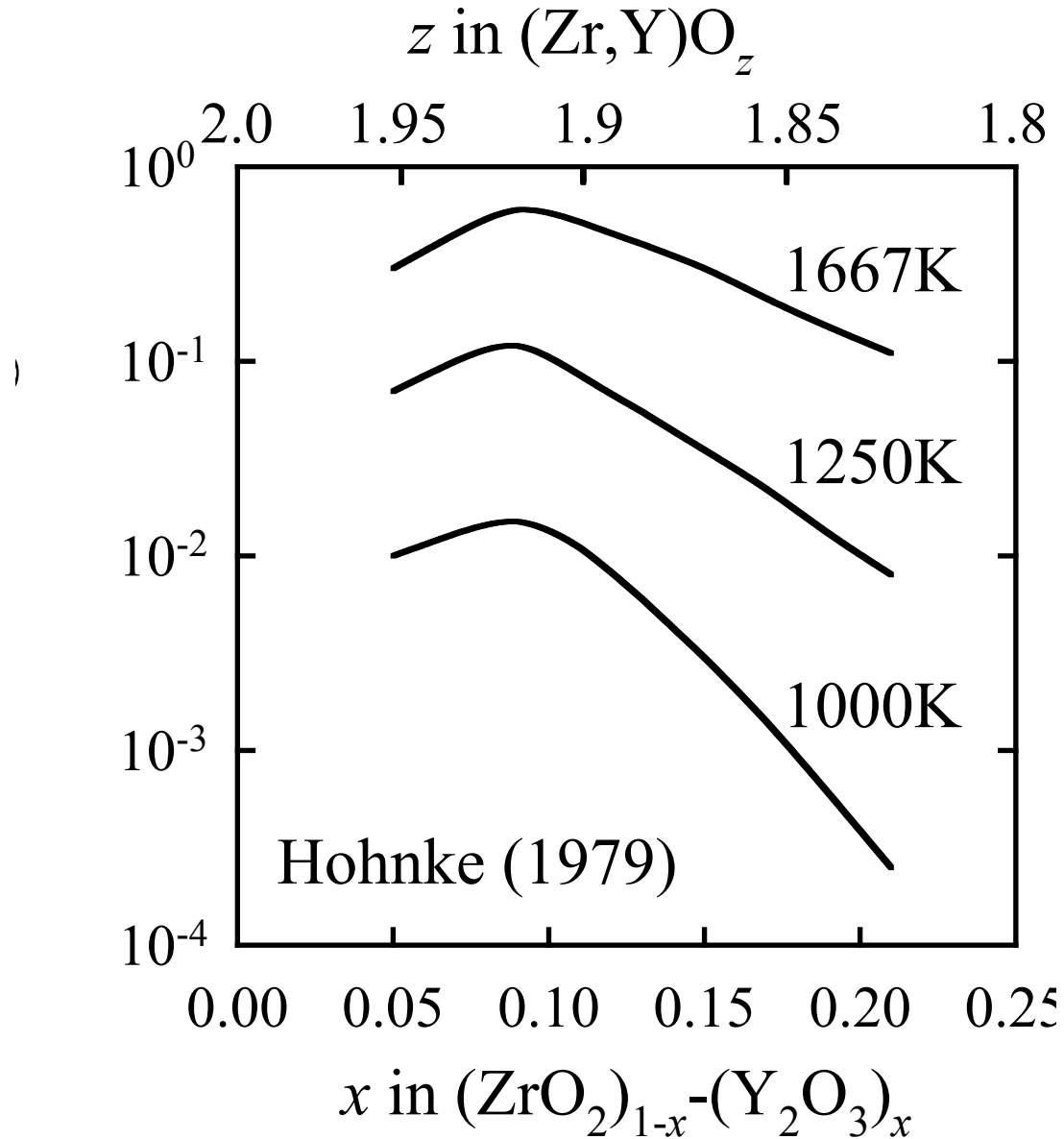
At  $T \sim 1370\text{K}$  it transforms to the tetragonal form ( $t\text{-ZrO}_2$ ,  $P4_2/nmc$ ) which has a slightly distorted fluorite structure.

At  $T \sim 2643\text{K}$  it transforms to the cubic fluorite structure ( $c\text{-ZrO}_2$ ) prior to melting at  $T \sim 2988\text{K}$ .

It is well known that the cubic form can be stabilised at ambient temperature ( $c^*\text{-ZrO}_2$ ) by the addition of divalent ( $\text{Ca}^{2+}$ ,  $\text{Mg}^{2+}$ , etc.) or trivalent ( $\text{Y}^{3+}$ ,  $\text{La}^{3+}$ , etc.) cations.

- The dopant cations sit substitutionally on the  $\text{Zr}^{4+}$  sites.
- Electrical neutrality maintained by vacancies on the anion sublattice.
- The  $\text{O}^{2-}$  vacancies cause displacements of the anions *and* cations.
- Presence of  $\text{O}^{2-}$  vacancies gives rise to high ionic conductivity  $\square$ .

# ZrO<sub>2</sub>-Y<sub>2</sub>O<sub>3</sub> : IONIC CONDUCTIVITY

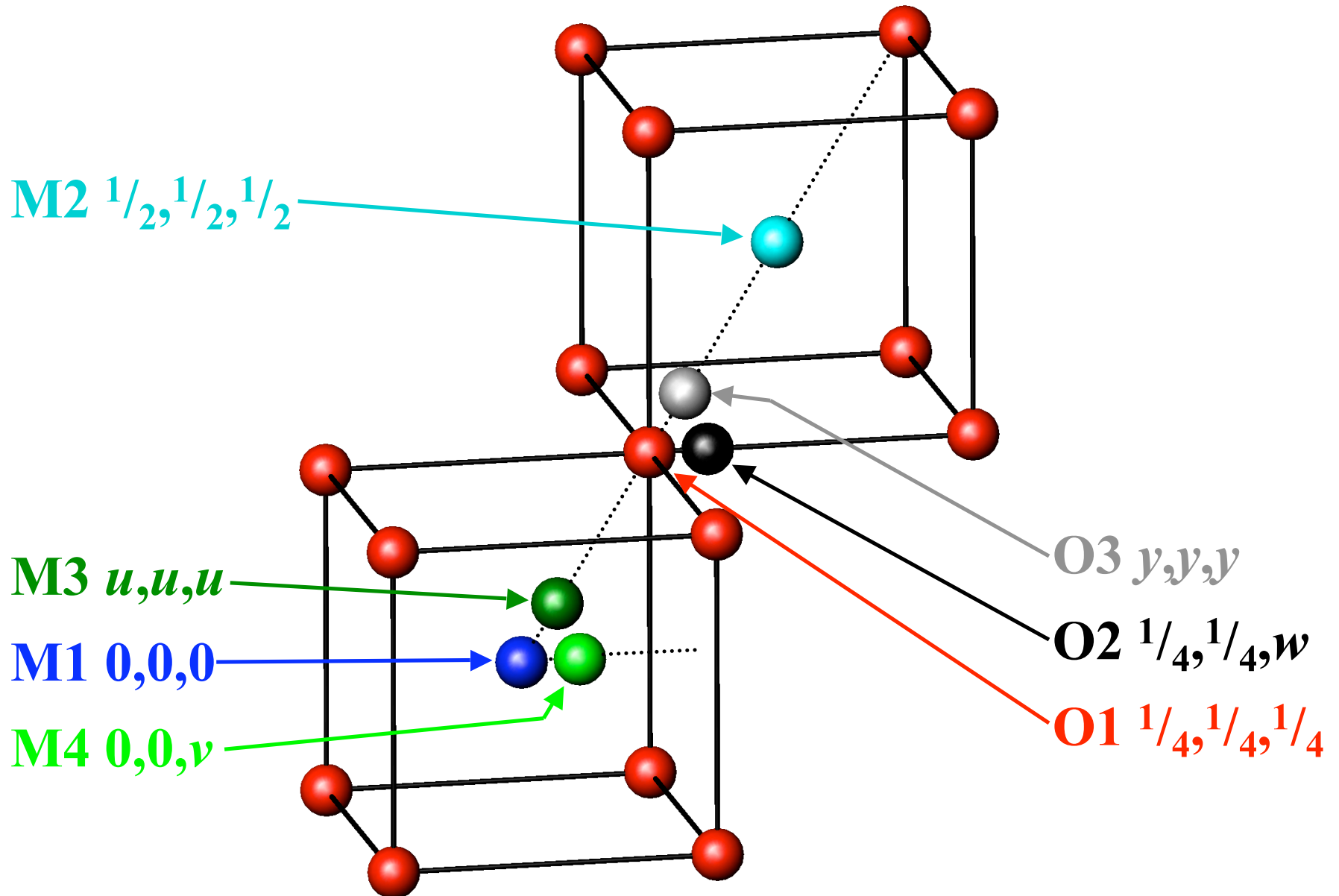


The ZrO<sub>2</sub>-Y<sub>2</sub>O<sub>3</sub> system is probably the most widely studied.

The ionic conductivity  $\sigma$  of  $(\text{ZrO}_2)_{1-x}-(\text{Y}_2\text{O}_3)_x$  reaches a maximum close to the lower stability limit of the  $c^*$ -ZrO<sub>2</sub> phase ( $x \sim 0.9$ ) and then falls rapidly with increasing  $x$ .

Numerous diffraction studies (neutron and X-ray) of  $(\text{ZrO}_2)_{1-x}-(\text{Y}_2\text{O}_3)_x$  have been performed.

# ZrO<sub>2</sub>-Y<sub>2</sub>O<sub>3</sub> : PROPOSED SITES



## ZrO<sub>2</sub>-Y<sub>2</sub>O<sub>3</sub> : DIFFRACTION RESULTS

Model	Description	R <sub>W</sub> (%)	
		x=0.100	x=0.184
I	Fluorite : <b>M1</b> cations + <b>O1</b> anions	2.87	2.48
IIa	Model I + <b>M2</b> cation interstitials	2.85	2.48
IIb	Model I + anion vacancies	2.43	2.22
IIIa	As IIb + <b>O2</b> anions relaxed in <001>	2.29	2.02
IIIb	As IIb + <b>O3</b> anions relaxed in <111>	2.37	2.15
IVa	As IIb + <b>M3</b> cations relaxed in <111>	2.17	1.74
IVb	As IIb + <b>M4</b> cations relaxed in <001>	2.42	2.19
V	<001> <b>O2</b> anions and <111> <b>M3</b> cations	2.01	1.44
Expected R-factor		R <sub>exp</sub> (%)	
		1.79	1.21

SXD time-of-flight diffractometer at ISIS Spallation Neutron Source.  
 $\sim 0.5 < \lambda (\text{\AA}) < \sim 8.5$ ,  $Q_{\max} \sim 18 \text{\AA}^{-1}$ ,  $\sim 180$  reflections ( $\sim 70$  independent).

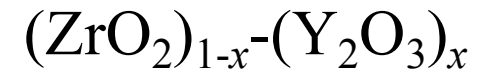
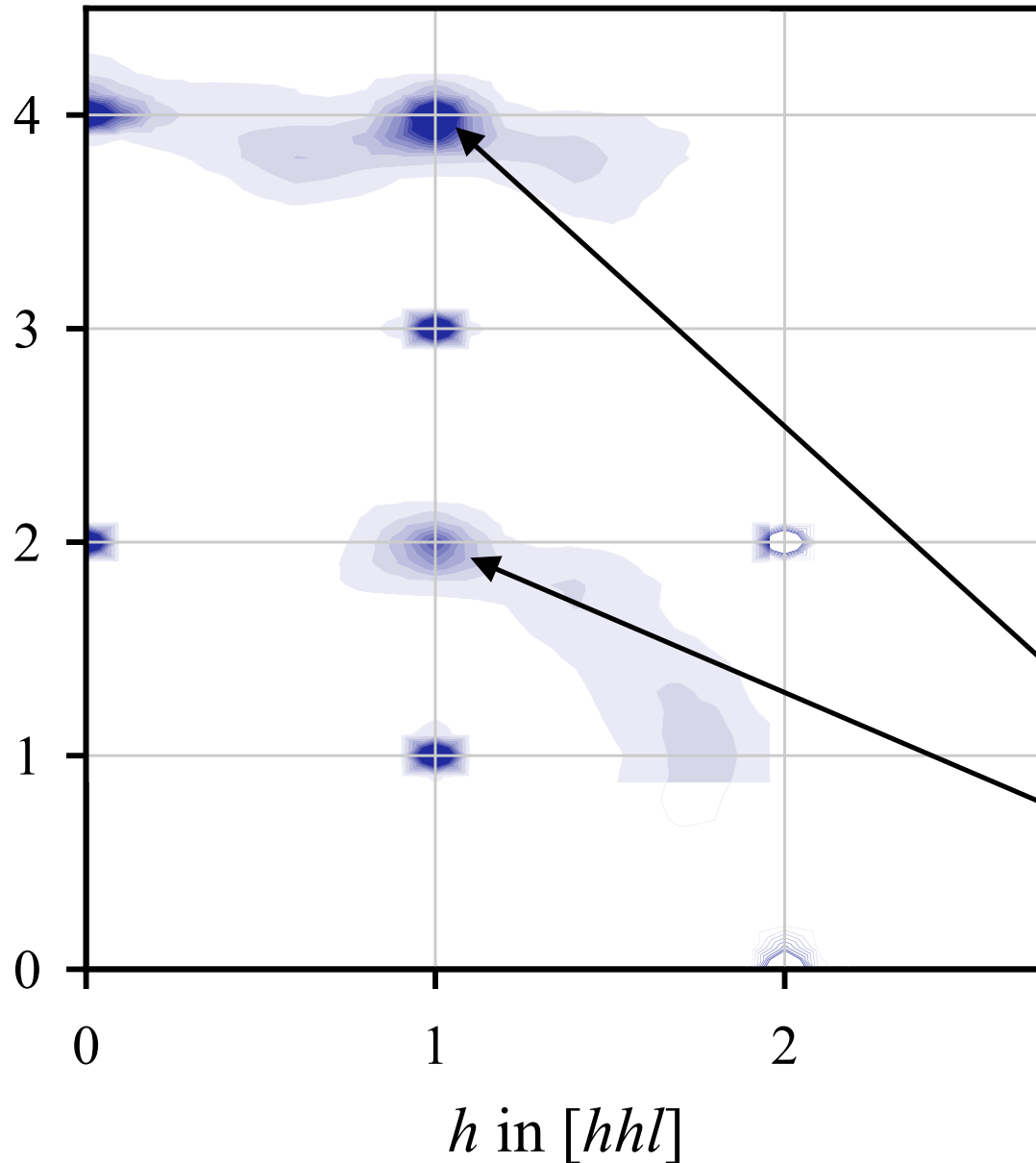
## ZrO<sub>2</sub>-Y<sub>2</sub>O<sub>3</sub> : DIFFRACTION RESULTS

Results obtained by fits to Bragg diffraction data using model V :

Parameter	Symbol	(Zr,Y)O <sub>1.910</sub>	(Zr,Y)O <sub>1.845</sub>
Scale factor	S	0.1522(7)	0.1717(6)
Cation thermal parameter	B <sub>M1</sub> =B <sub>M2</sub>	0.24(5)	0.32(7)
Lattice cation occupancy	n <sub>M1</sub>	0.71(8)	0.55(7)
Relaxed cation occupancy	n <sub>M3</sub>	0.29(8)	0.45(7)
Relaxed cation position	<i>u</i> in <i>u,u,u</i>	0.028(2)	0.031(2)
Anion thermal parameter	B <sub>O1</sub> =B <sub>O2</sub>	0.61(4)	0.55(3)
Lattice anion occupancy	n <sub>O1</sub>	1.2(1)	0.8(1)
Relaxed anion occupancy	n <sub>O2</sub>	0.7(1)	1.0(1)
Relaxed anion position	<i>w</i> in <sup>1</sup> / <sub>4</sub> , <sup>1</sup> / <sub>4</sub> , <i>w</i>	0.294(2)	0.291(2)

The site occupancies are not determined with sufficient accuracy to select correct defect structure(s) □ consider the diffuse scattering.....

# ZrO<sub>2</sub>-Y<sub>2</sub>O<sub>3</sub> : DIFFUSE SCATTERING



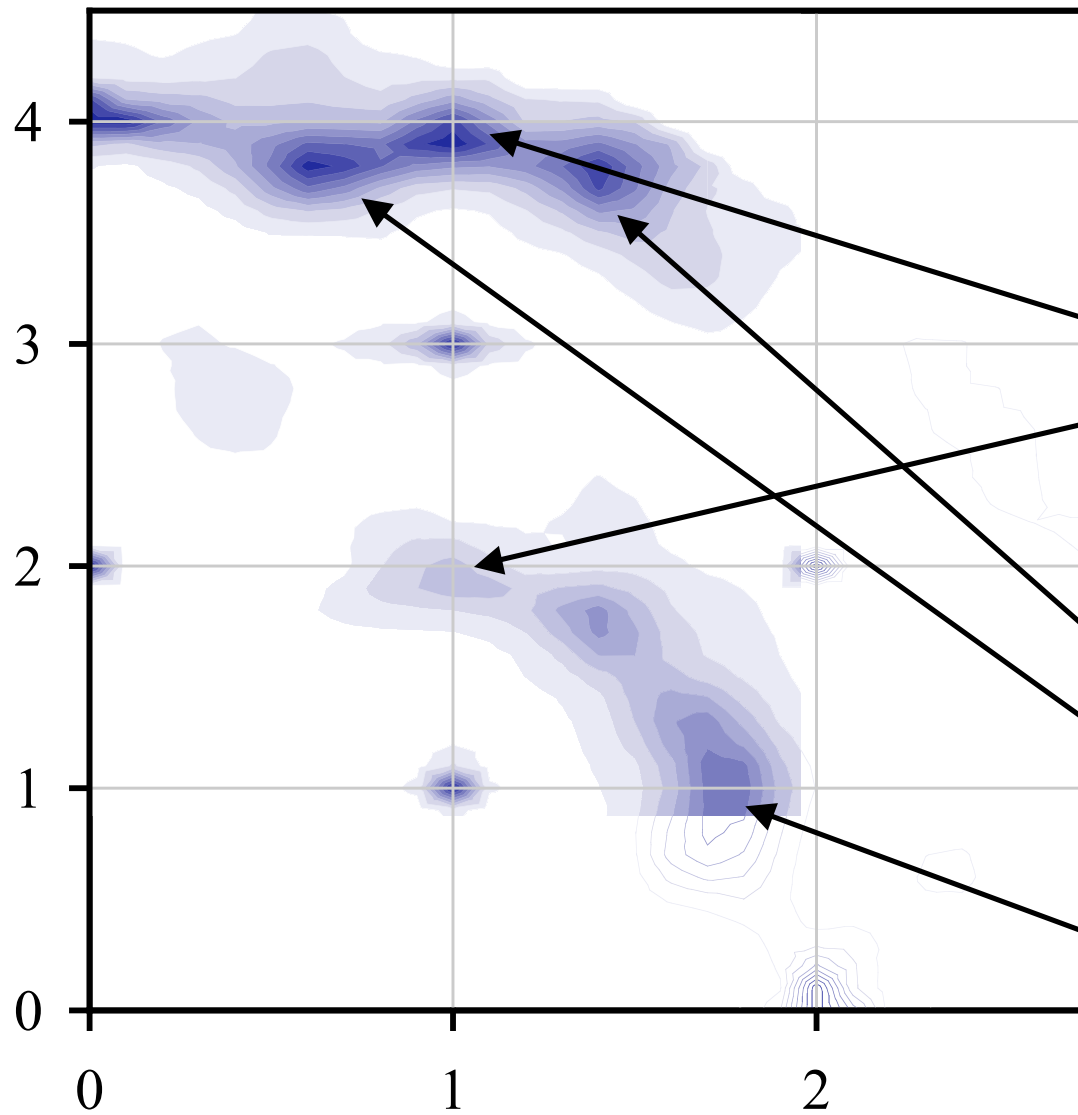
$x=0.100(4)$

$h$ - $hl$  plane

*f.c.c.* Bragg peaks :  
002, 004, 111, 113,  
220, 222, *etc.*

Also diffuse peaks at  
'forbidden' positions  
112 and 114.

# ZrO<sub>2</sub>-Y<sub>2</sub>O<sub>3</sub> : DIFFUSE SCATTERING



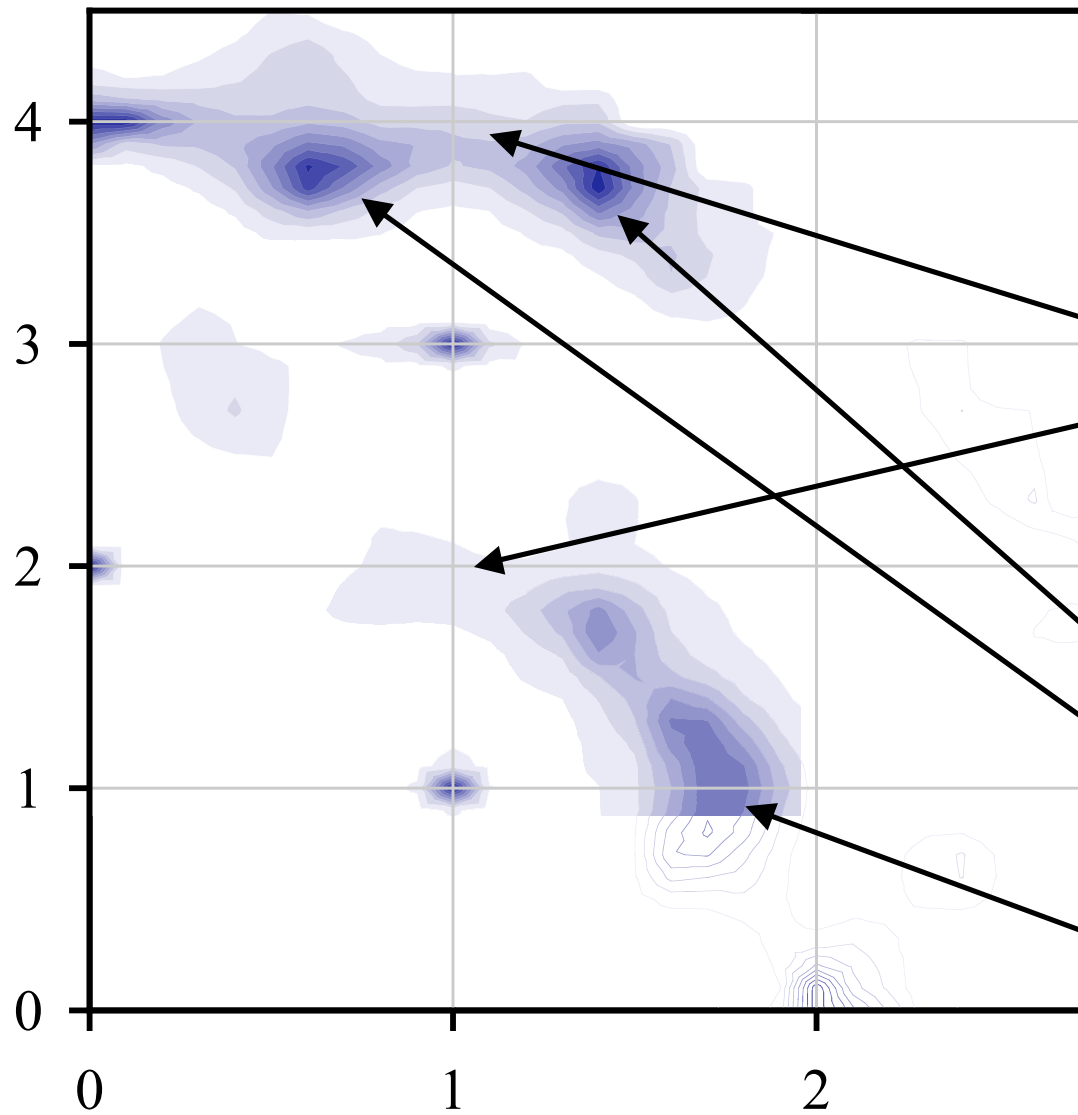
$(\text{ZrO}_2)_{1-x}-(\text{Y}_2\text{O}_3)_x$   
 $x=0.126(5)$

Diffuse peaks at  
 $\underline{Q}=1,1,2$  and  $\underline{Q}=1,1,4$   
decrease in intensity.

New peaks appear :  
 $\underline{Q}\sim 1.4, 1.4, 3.8,$   
 $\underline{Q}\sim 0.6, 0.6, 3.8,$  etc.

Also broad intensity  
at  $\underline{Q}\sim 1.7, 1.7, 1.0$

# ZrO<sub>2</sub>-Y<sub>2</sub>O<sub>3</sub> : DIFFUSE SCATTERING



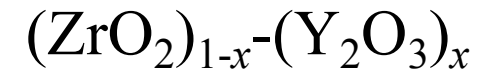
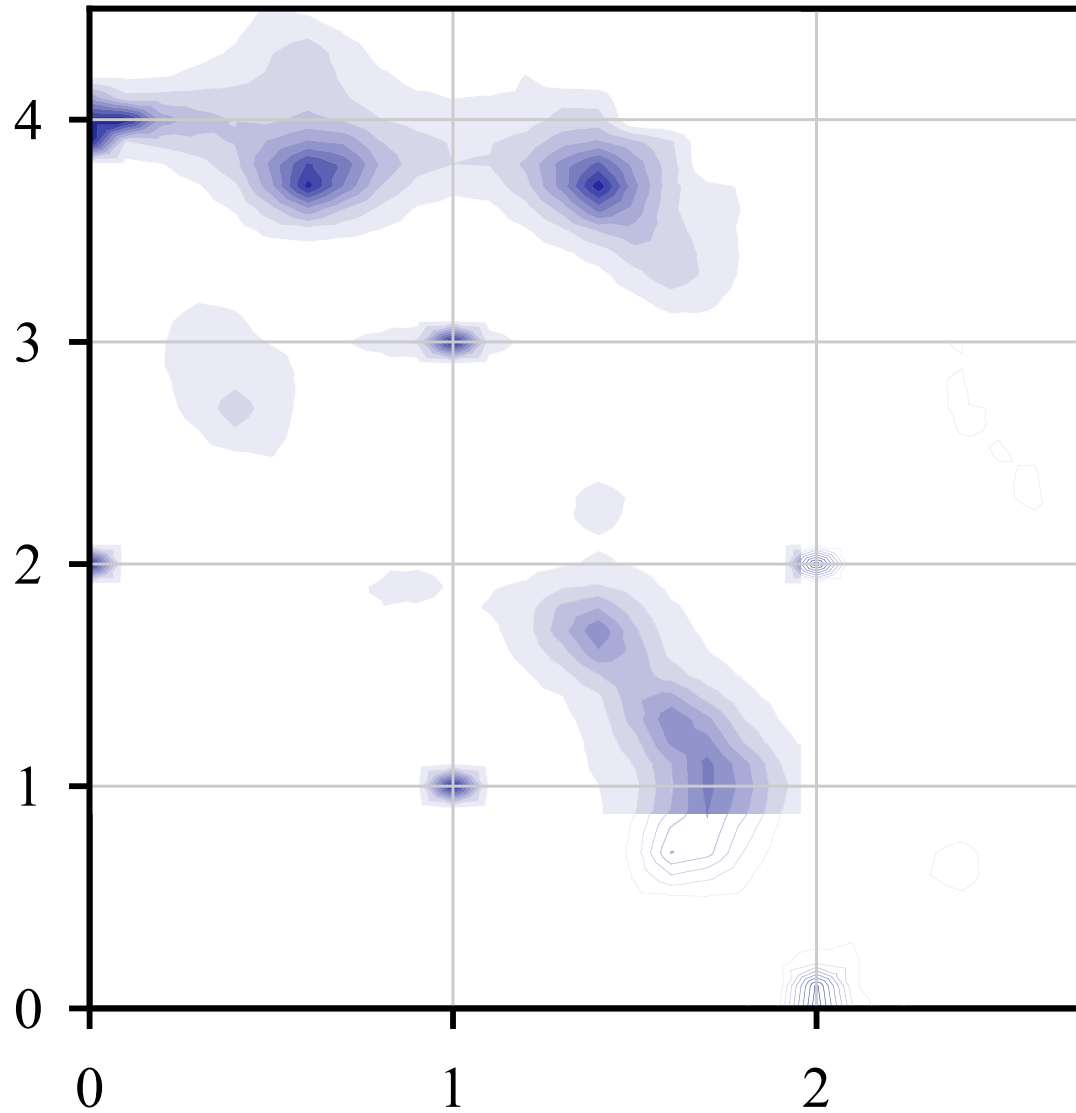
$(\text{ZrO}_2)_{1-x}-(\text{Y}_2\text{O}_3)_x$   
 $x=0.158(6)$

Diffuse peaks at  $\underline{Q}=1,1,2$  and  $\underline{Q}=1,1,4$  disappeared.

$\underline{Q}\sim 1.4,1.4,3.8$  and  $\underline{Q}\sim 0.6,0.6,3.8$  peaks increase in intensity.

Broad feature at  $\underline{Q}\sim 1.7,1.7,1.0$  also increases in intensity.

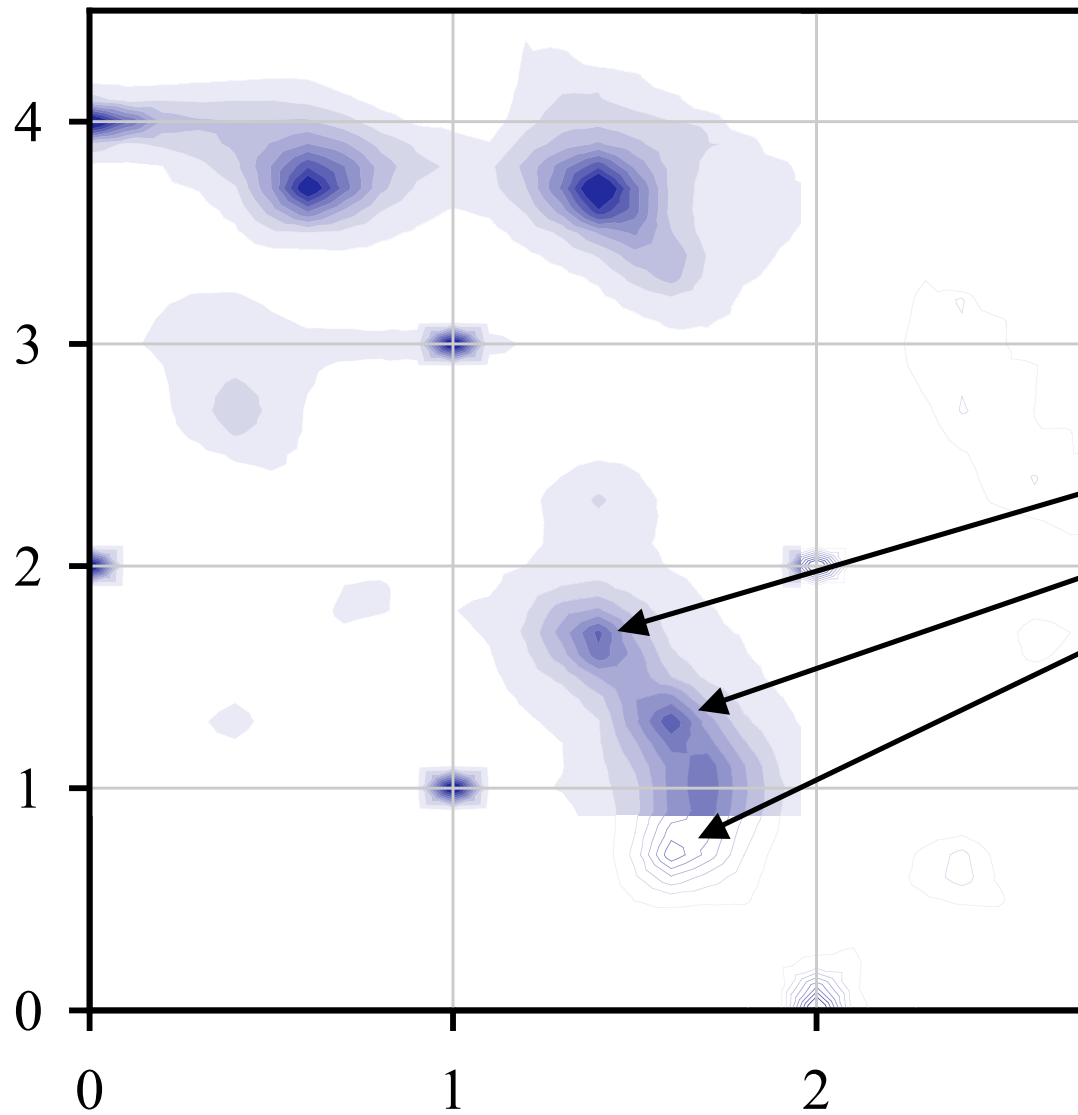
# ZrO<sub>2</sub>-Y<sub>2</sub>O<sub>3</sub> : DIFFUSE SCATTERING



$$x=0.184(7)$$

Same trends.

# ZrO<sub>2</sub>-Y<sub>2</sub>O<sub>3</sub> : DIFFUSE SCATTERING



$(\text{ZrO}_2)_{1-x}-(\text{Y}_2\text{O}_3)_x$   
 $x=0.221(9)$

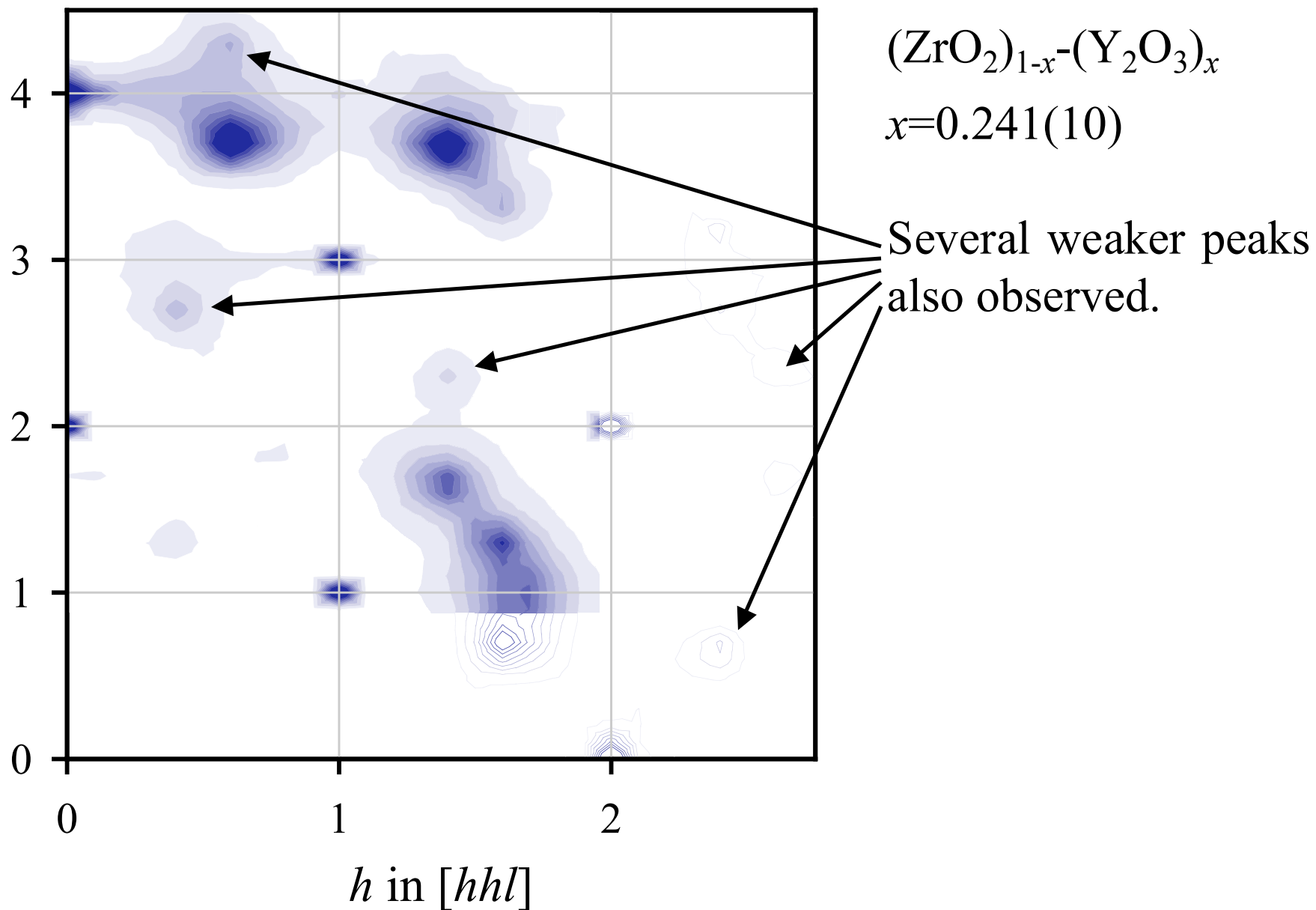
Additional peaks  
appear at :

$Q \sim 1.4, 1.4, 1.8,$

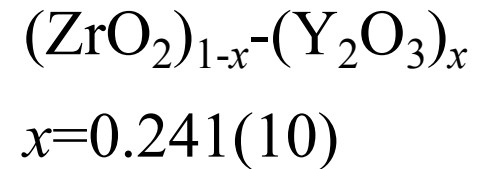
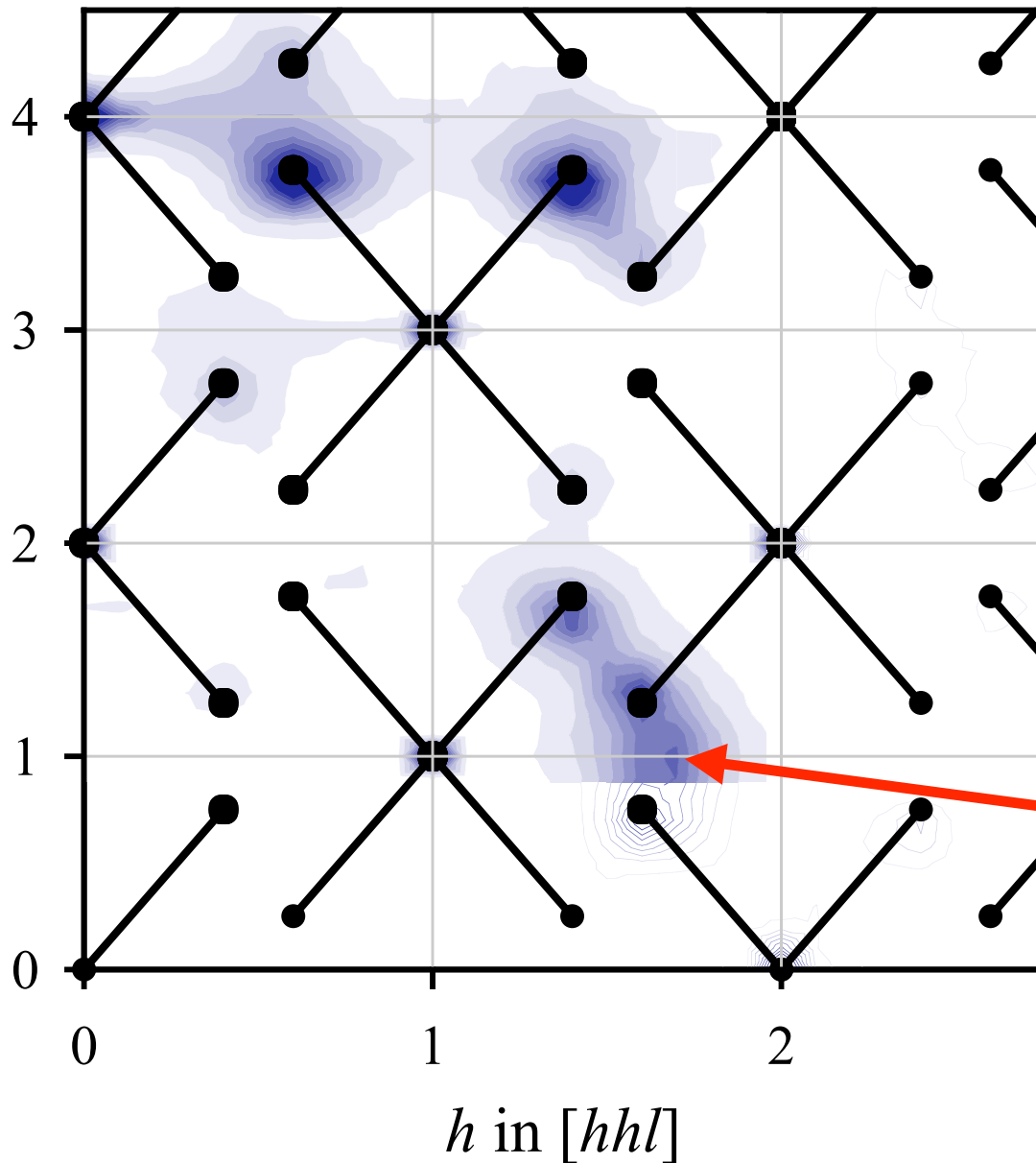
$Q \sim 1.6, 1.6, 1.2,$

$Q \sim 1.6, 1.6, 0.8, \text{ etc.}$

# ZrO<sub>2</sub>-Y<sub>2</sub>O<sub>3</sub> : DIFFUSE SCATTERING



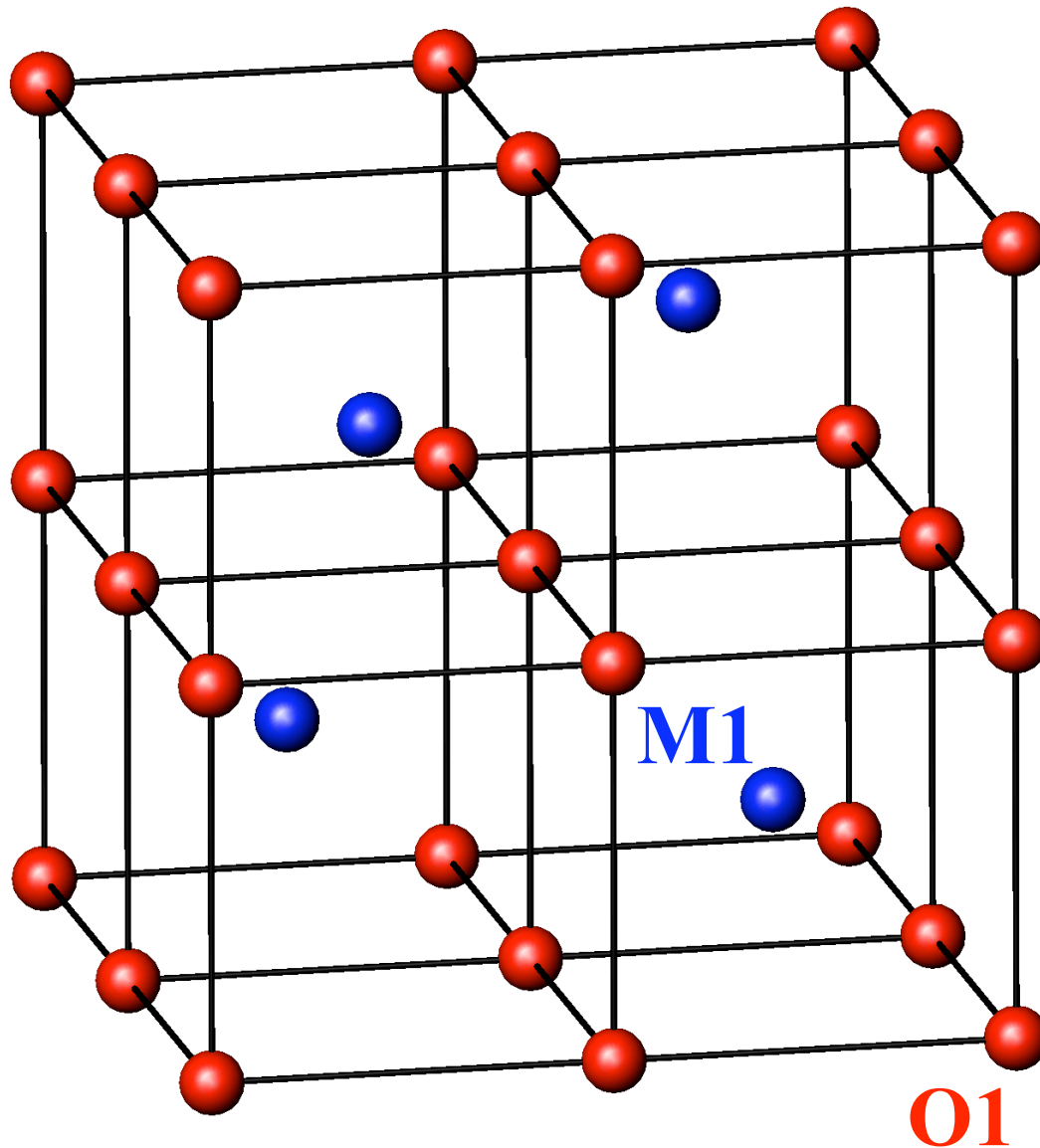
# ZrO<sub>2</sub>-Y<sub>2</sub>O<sub>3</sub> : DIFFUSE SCATTERING



The diffuse peaks can be considered as 'superlattice' peaks at  $\underline{q}=\pm(0.4,0.4,\pm 0.8)$  with respect to the *f.c.c.* positions.

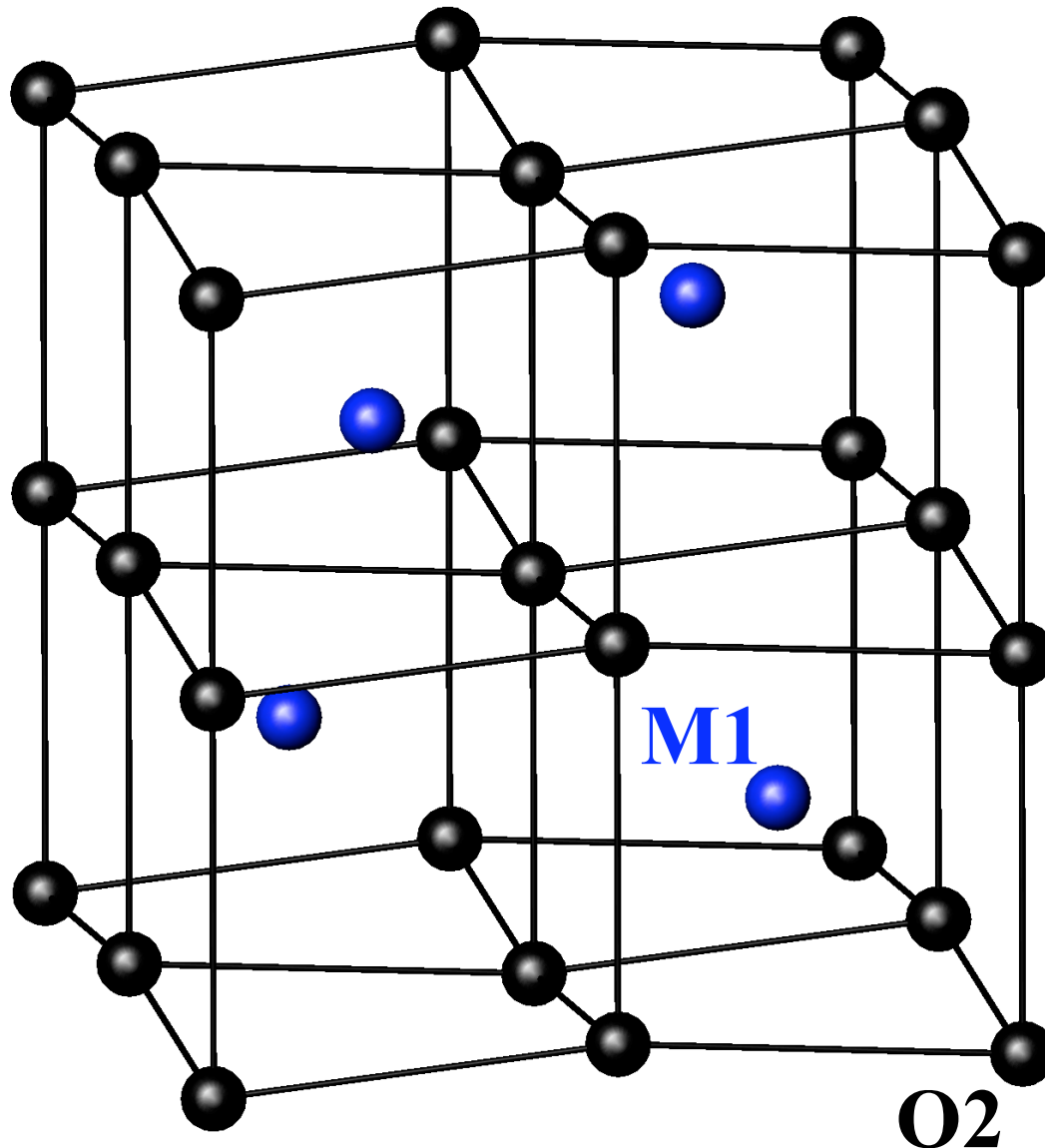
Broad intensity at  $\underline{Q}\sim 1.7,1.7,1.0$  has a different origin.

# ZrO<sub>2</sub>-Y<sub>2</sub>O<sub>3</sub> : TETRAGONAL DISTORTION



Diffuse peaks are observed at  $Q \sim 1,1,2$  and  $Q \sim 1,1,4$  at low  $x$  values.

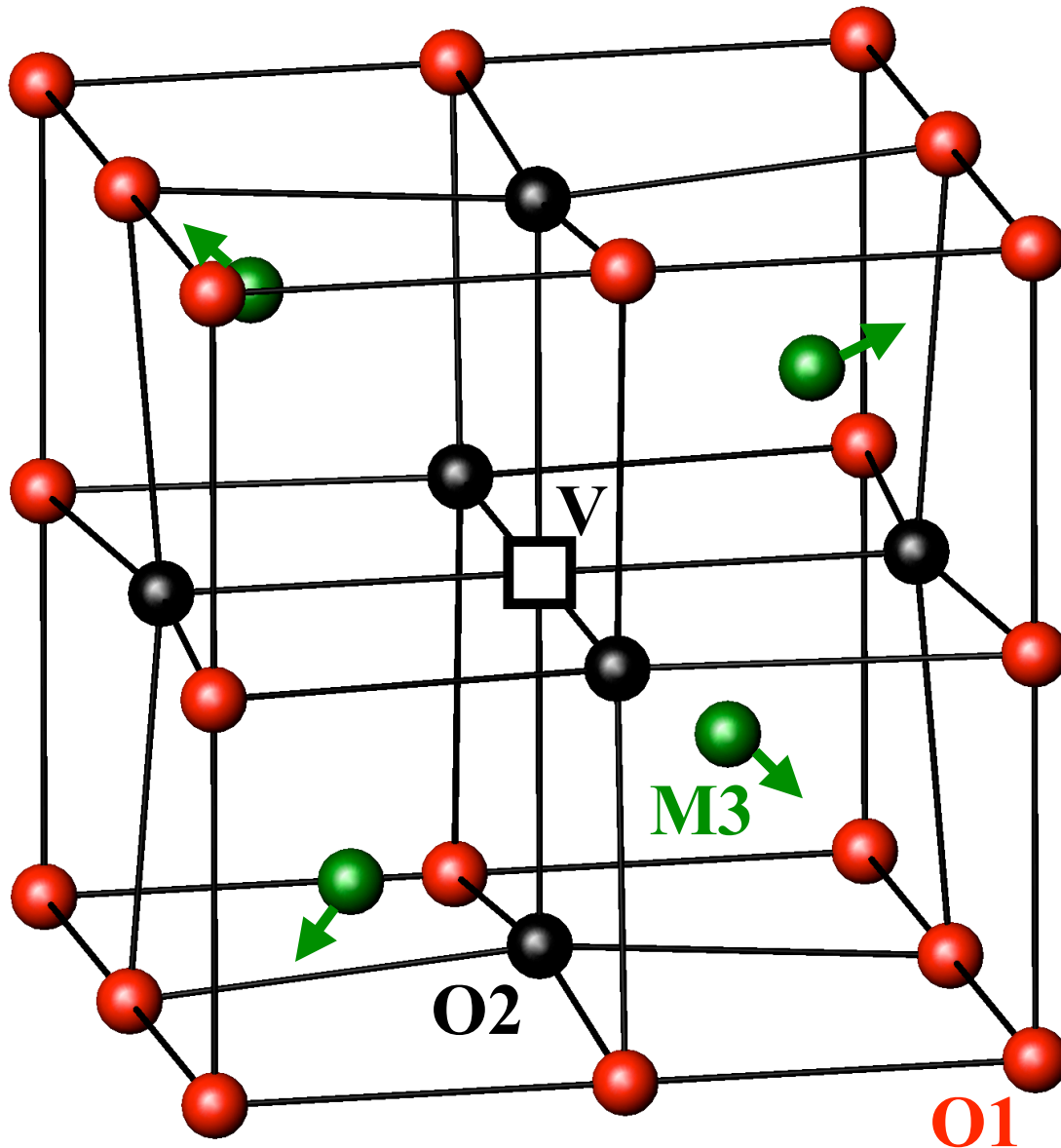
# ZrO<sub>2</sub>-Y<sub>2</sub>O<sub>3</sub> : TETRAGONAL DISTORTION



Diffuse peaks are observed at  $Q \sim 1,1,2$  and  $Q \sim 1,1,4$  at low  $x$  values.

These arise from small regions of the crystal (around 20Å in size) undergoing a slight tetragonal distortion, of the type observed in the  $t$  - ZrO<sub>2</sub> phase.

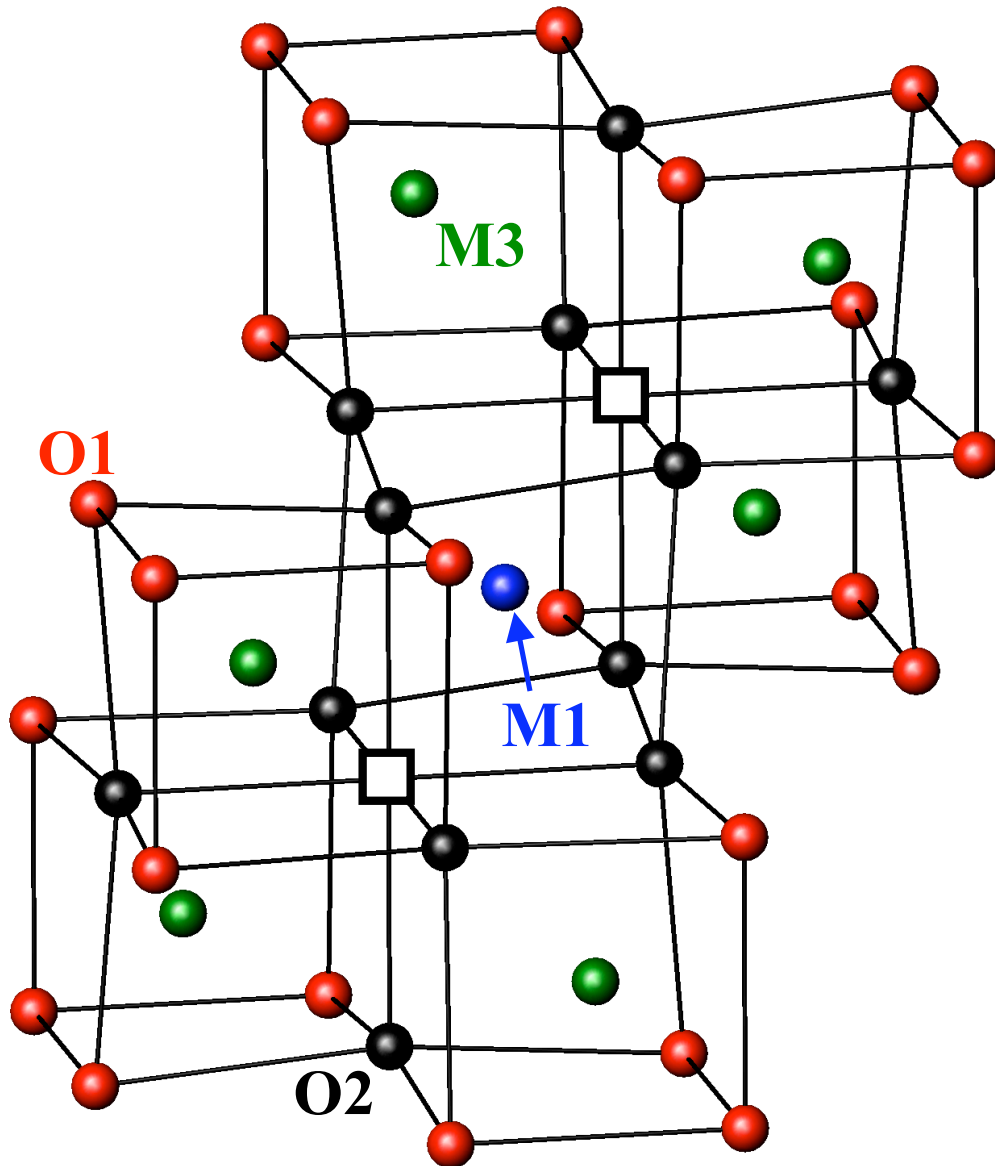
## ZrO<sub>2</sub>-Y<sub>2</sub>O<sub>3</sub> : SINGLE VACANCIES



Simulations of the diffuse scattering suggest that the broad peak located at  $Q \sim 1.7, 1.7, 1.0$  arises from isolated O<sup>2-</sup> vacancies (V).

Neighbouring anions are relaxed in  $\langle 100 \rangle$  towards the vacancy (forming **O2** sites) and nearest cations are relaxed in  $\langle 111 \rangle$  away from the vacancy (into **M3** sites).

# ZrO<sub>2</sub>-Y<sub>2</sub>O<sub>3</sub> : VACANCY CLUSTERS

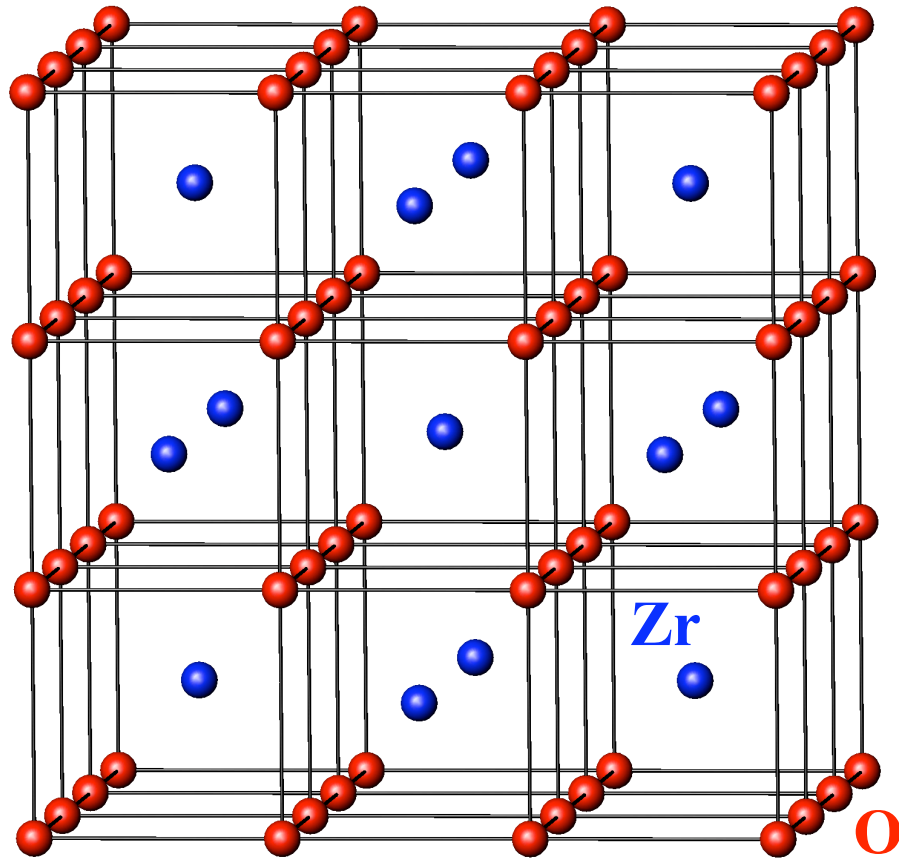


The third type of defect present are vacancy pairs with relaxations of surrounding anions (to **O2**) and cations (to **M3**).

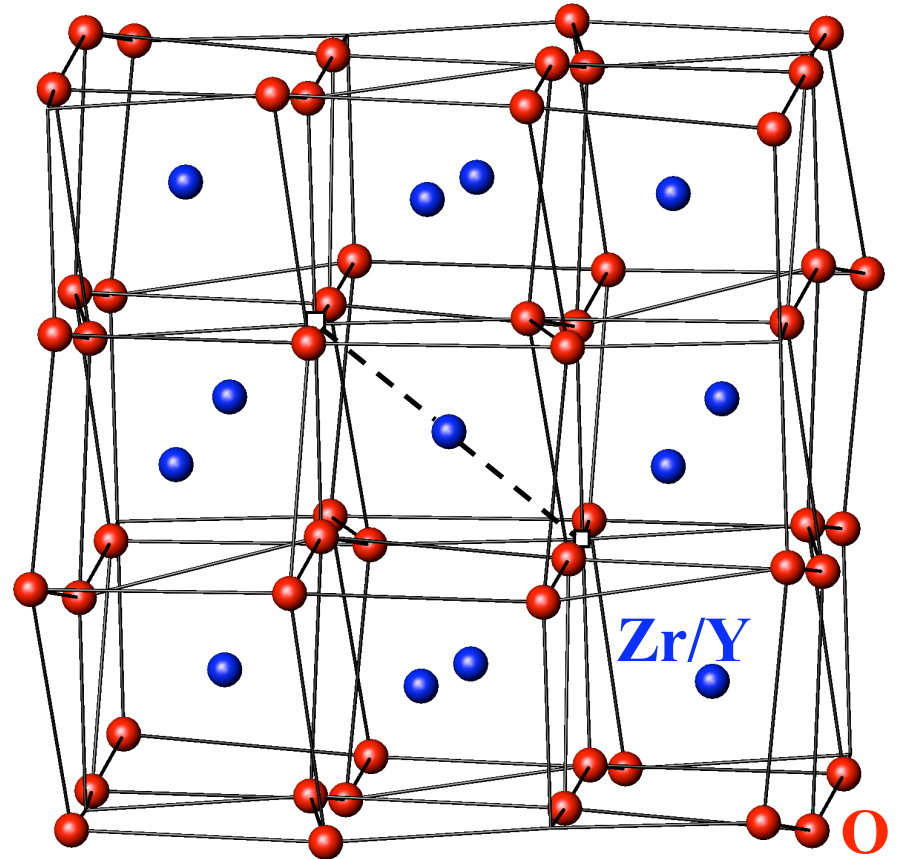
The O<sup>2-</sup> vacancy pairs are in  $\langle 111 \rangle$  directions, with an **M1** cation between.

These units form larger clusters ( $\sim 15\text{\AA}$ ), separated by  $(1, -1/2, 1/2)$  fluorite vectors and give rise to the observed diffuse peaks at  $q=0.4, 0.4, 0.8$ .

# $\text{Zr}_3\text{Y}_4\text{O}_{12}$ : CRYSTAL STRUCTURE



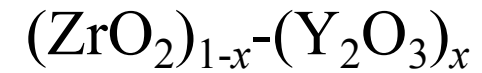
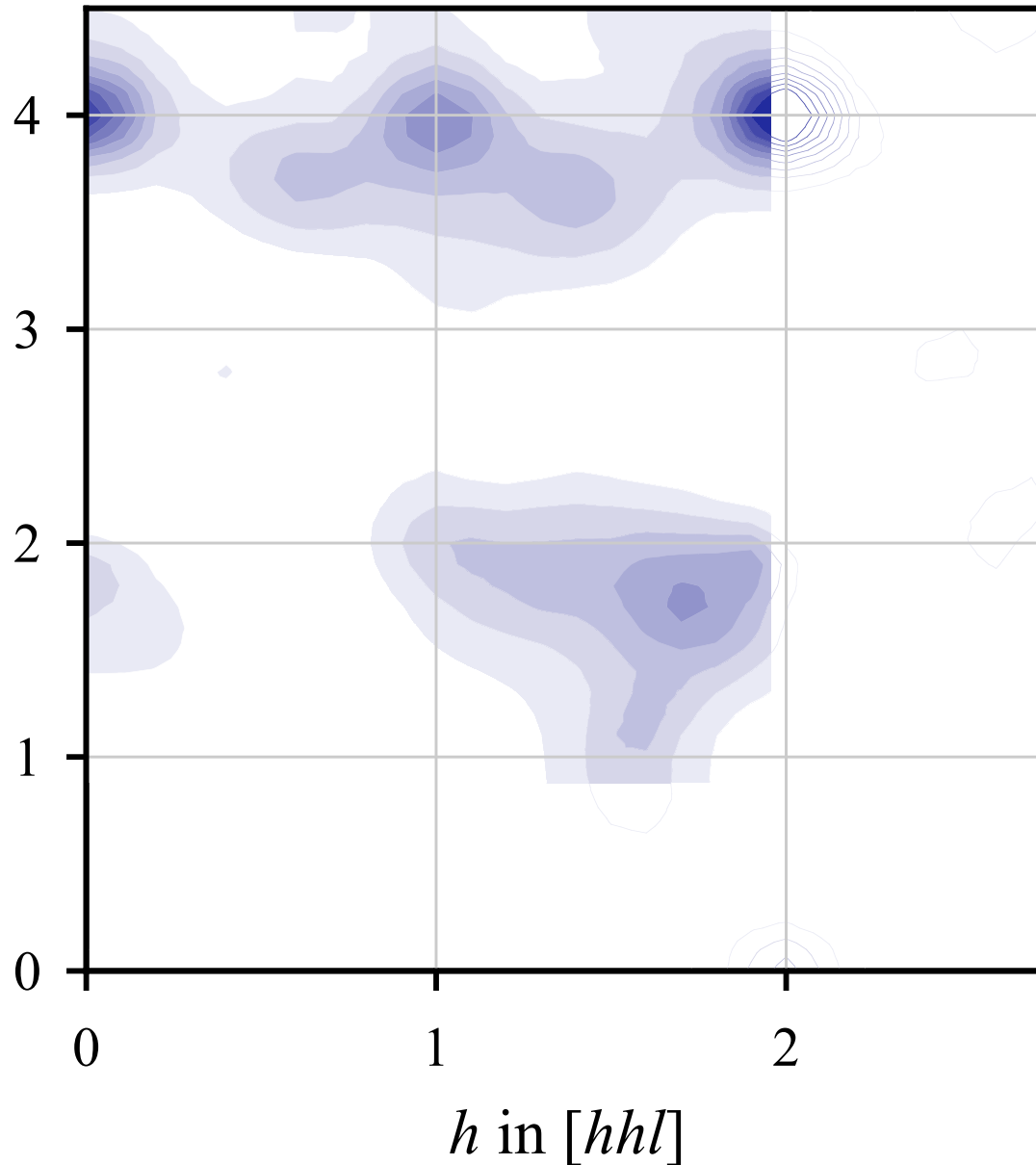
$c\text{-ZrO}_2$



$\text{Zr}_3\text{Y}_4\text{O}_{12}$

$\langle 111 \rangle$  vacancy pairs are a common structural feature within anion-deficient fluorites, including  $\text{Zr}_3\text{Y}_4\text{O}_{12}$  (*i.e.* the  $x=0.4$  compound).

# ZrO<sub>2</sub>-Y<sub>2</sub>O<sub>3</sub> : DIFFUSE SCATTERING

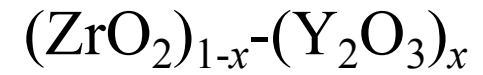
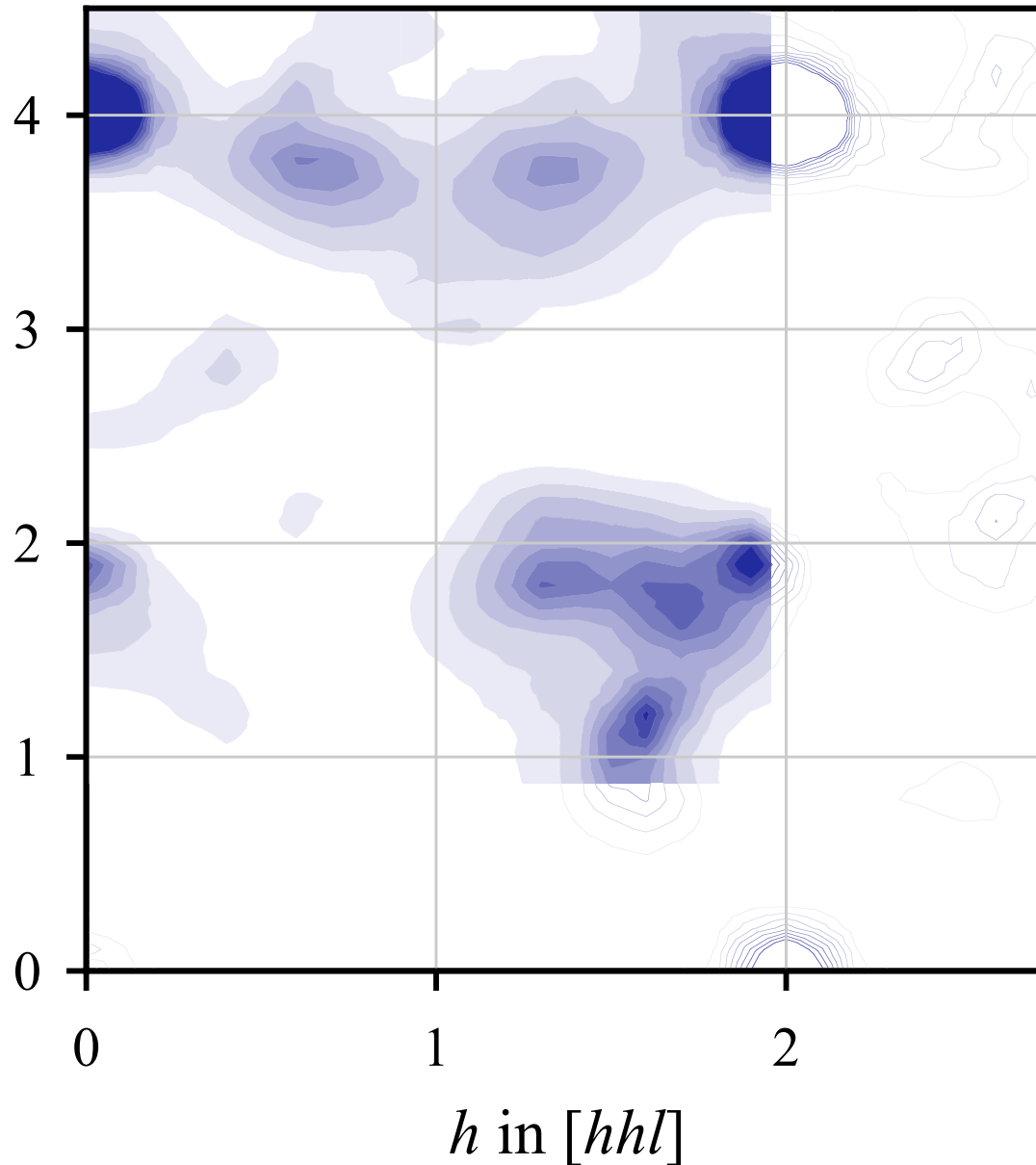


$$x \sim 0.1$$

Calculations of the diffuse scattering have been made, using the three defect models.

At  $x \sim 0.1$  the tetragonal distortion ( $Q \sim 1, 1, 4$ ) and the isolated vacancy types ( $Q \sim 1.7, 1.7, 1.0$ ) are most significant.

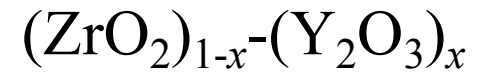
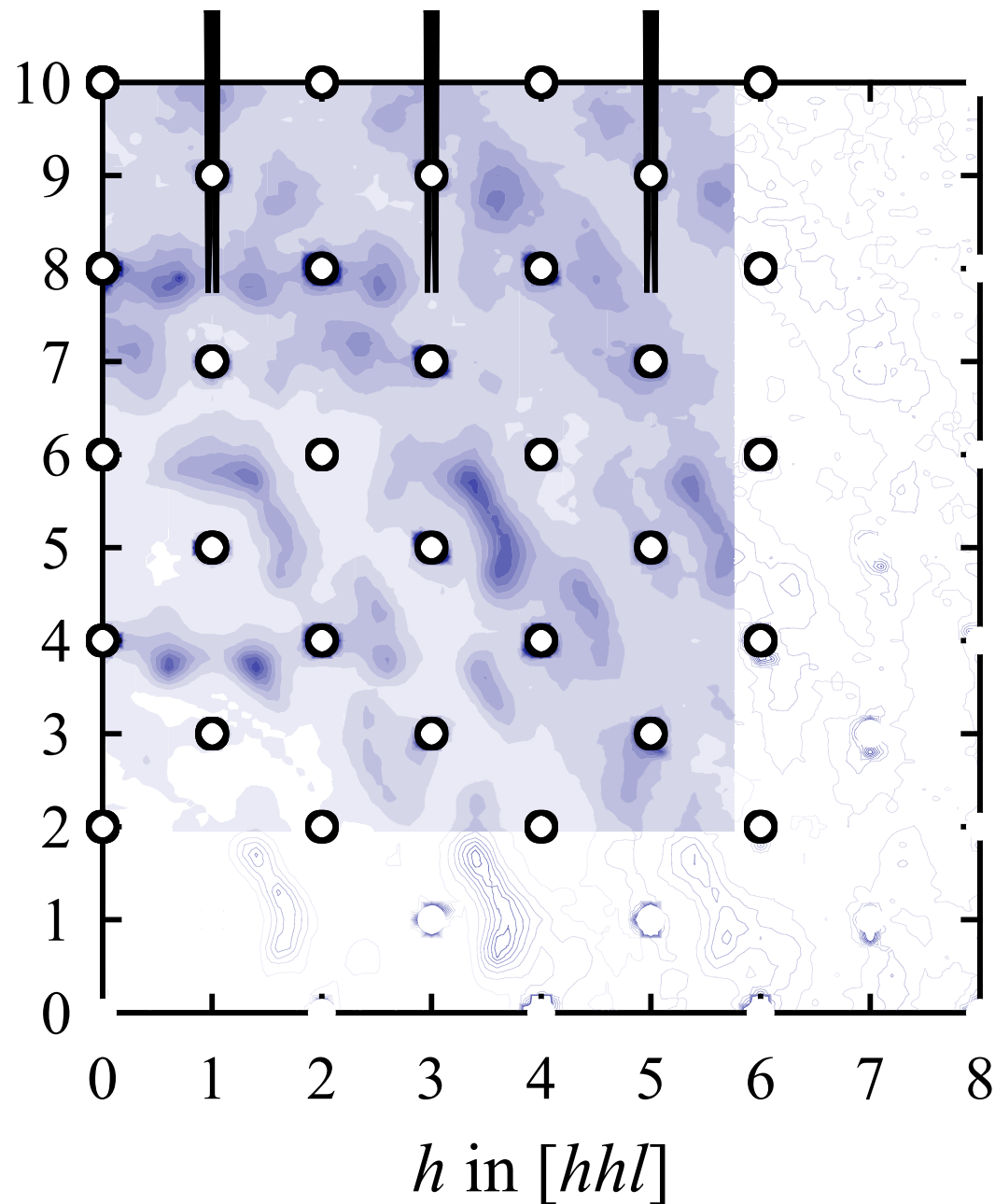
# ZrO<sub>2</sub>-Y<sub>2</sub>O<sub>3</sub> : DIFFUSE SCATTERING



$$x \sim 0.25$$

At  $x \sim 0.25$  the aggregates of  $\langle 111 \rangle$  vacancy pairs (the  $q=0.4, 0.4, 0.8$  peaks) and isolated vacancy units ( $Q \sim 1.7, 1.7, 1.0$ ) tend to dominate.

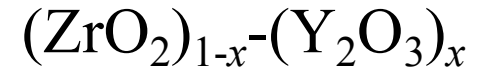
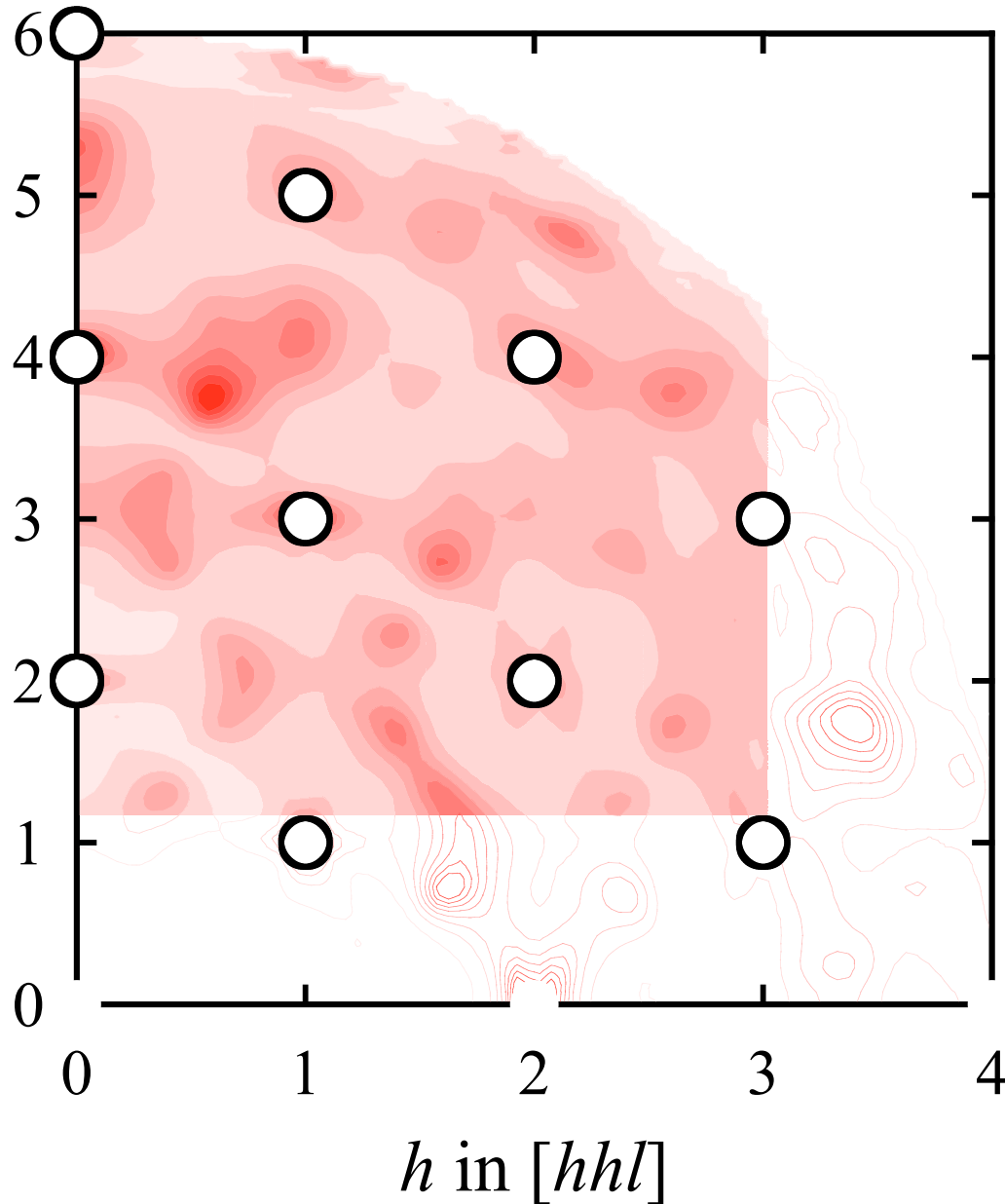
# ZrO<sub>2</sub>-Y<sub>2</sub>O<sub>3</sub> : DIFFUSE SCATTERING



$$x=0.184(7)$$

Diffuse scattering data measured to higher  $Q$  using SXD at ISIS is consistent with proposed model of defect structure of ZrO<sub>2</sub>-Y<sub>2</sub>O<sub>3</sub>.

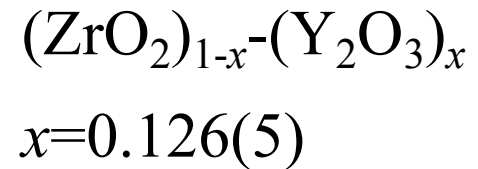
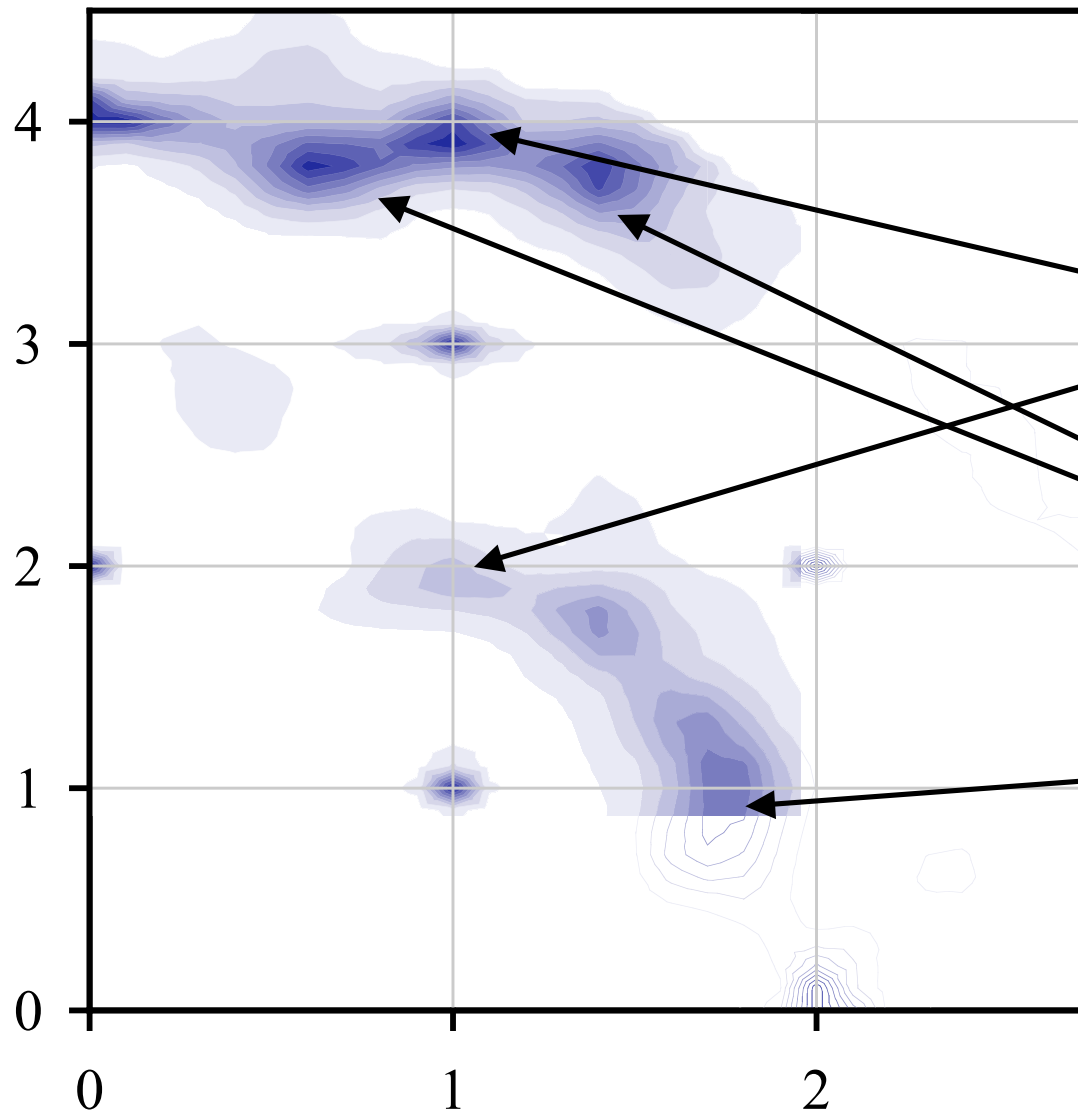
# ZrO<sub>2</sub>-Y<sub>2</sub>O<sub>3</sub> : DIFFUSE SCATTERING



$$x=0.184(7)$$

Diffuse X-ray scattering data has also been measured, to exploit the difference in relative scattering powers of the cations and anions for neutrons and X-rays.

# ZrO<sub>2</sub>-Y<sub>2</sub>O<sub>3</sub> : DIFFUSE SCATTERING



Peaks due to tetragonal distortion.

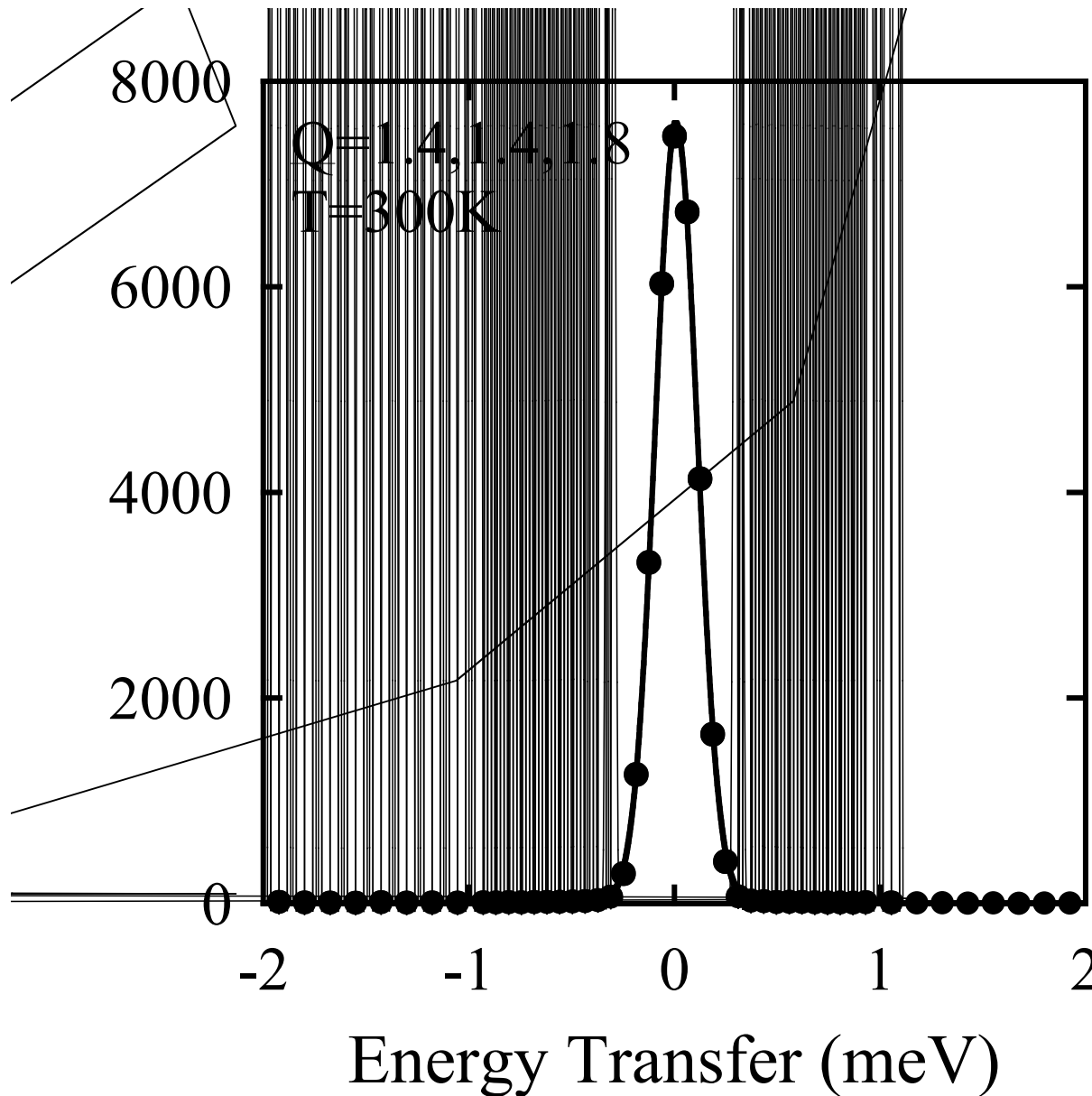
'Superlattice' peaks due to aggregates of  $\langle 111 \rangle$  vacancy pairs.

Broad intensity from isolated vacancies.

□ Look at energy broadening of diffuse scattering at each  $\underline{Q}$ .

$h$  in  $[hhl]$

# ZrO<sub>2</sub>-Y<sub>2</sub>O<sub>3</sub> : QUASIELASTIC SCATTERING



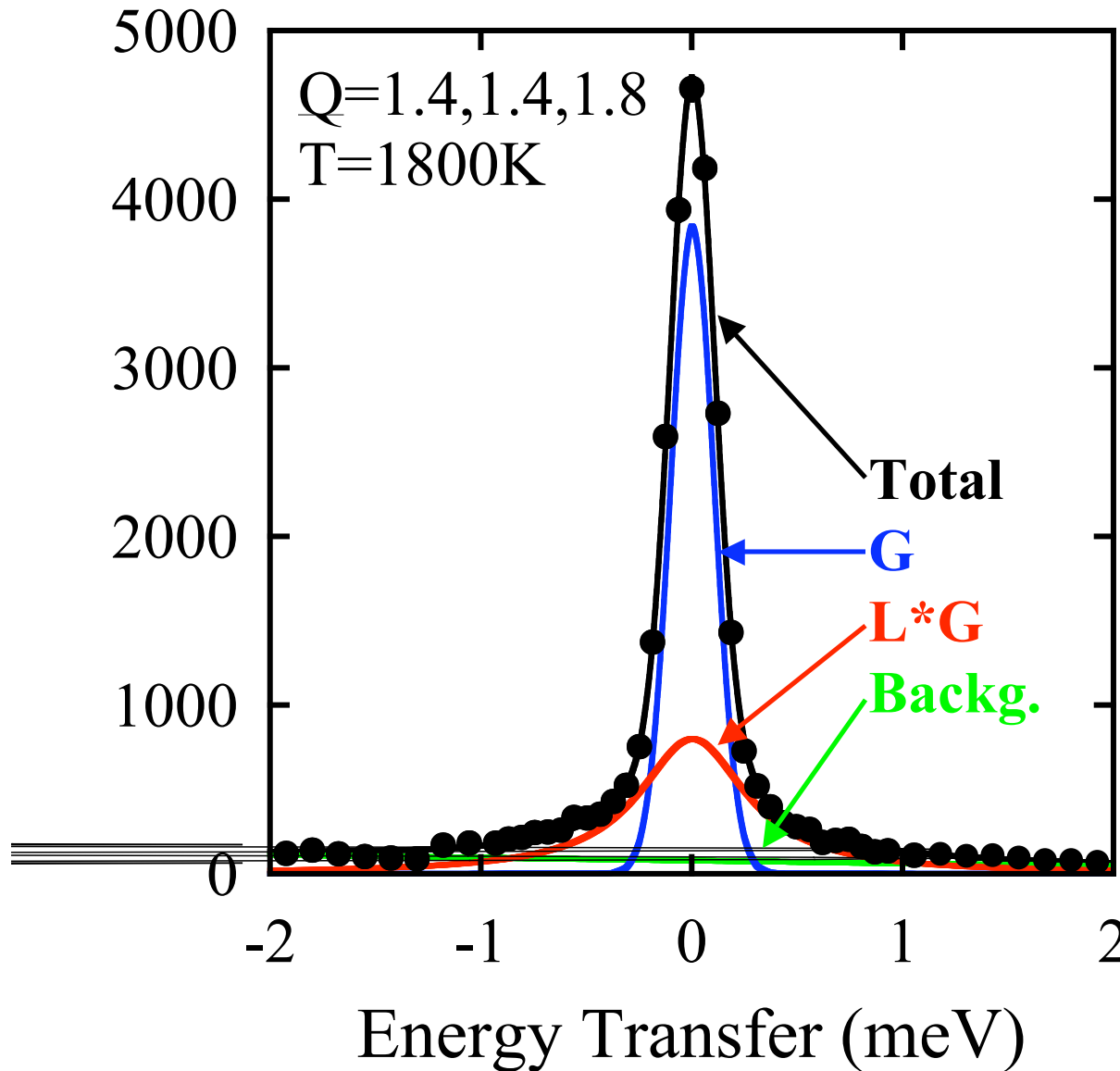
$x=0.126(5)$  sample.

At ambient T the diffuse scattering at all  $Q$  positions is elastic.

i.e. Gaussian profile in energy transfer of FWHM equal to the instrumental resolution).

□ all defects are static.

# ZrO<sub>2</sub>-Y<sub>2</sub>O<sub>3</sub> : QUASIELASTIC SCATTERING

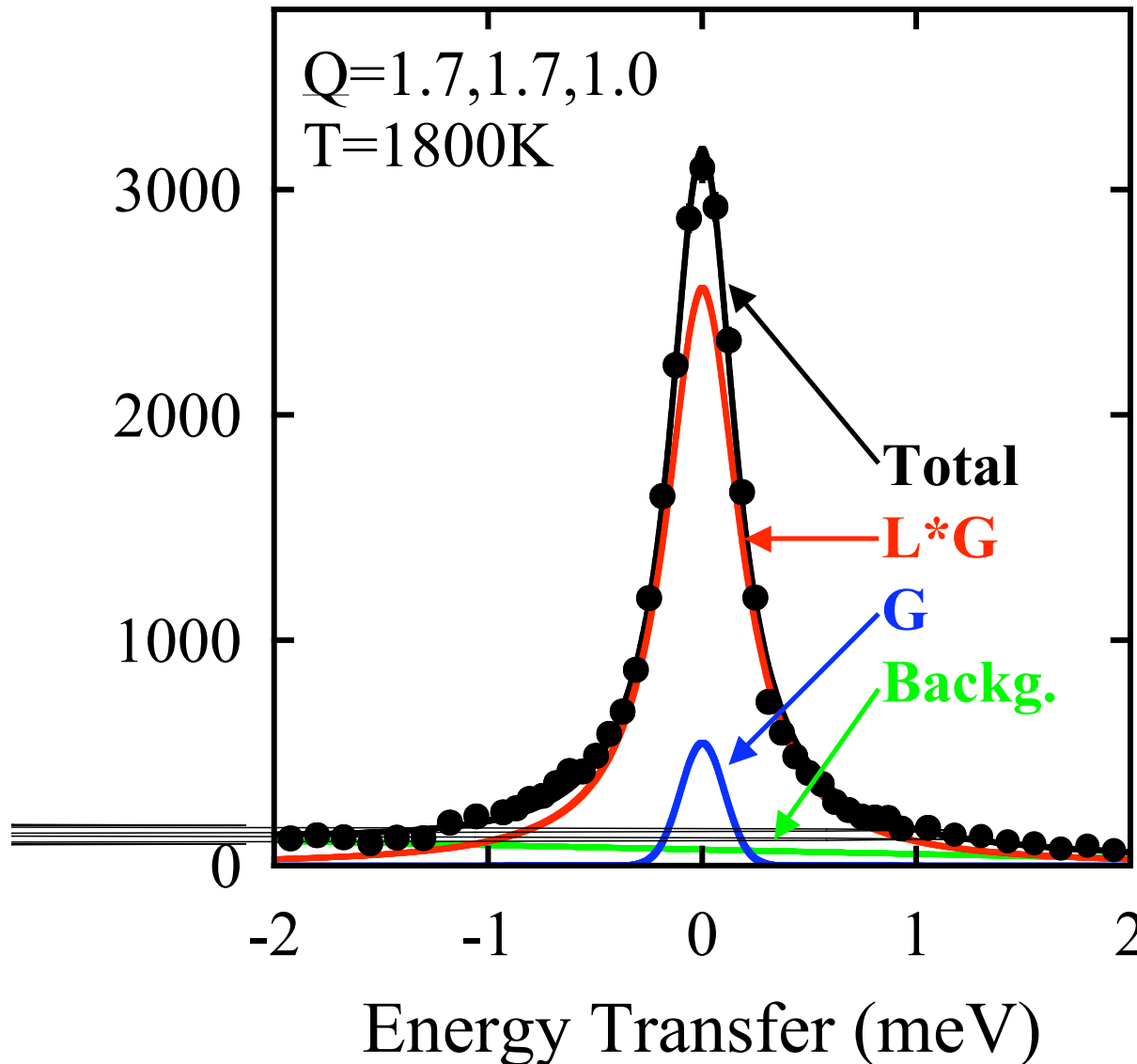


$x=0.126(5)$  sample.

At high T the diffuse scattering at the  $q=0.4, 0.4, 0.8$  peaks is still predominantly elastic (**G**), with only a small energy broadened Lorentzian component (**L\*G**).

□ the vacancy pair aggregates remain static at high temperature.

# ZrO<sub>2</sub>-Y<sub>2</sub>O<sub>3</sub> : QUASIELASTIC SCATTERING

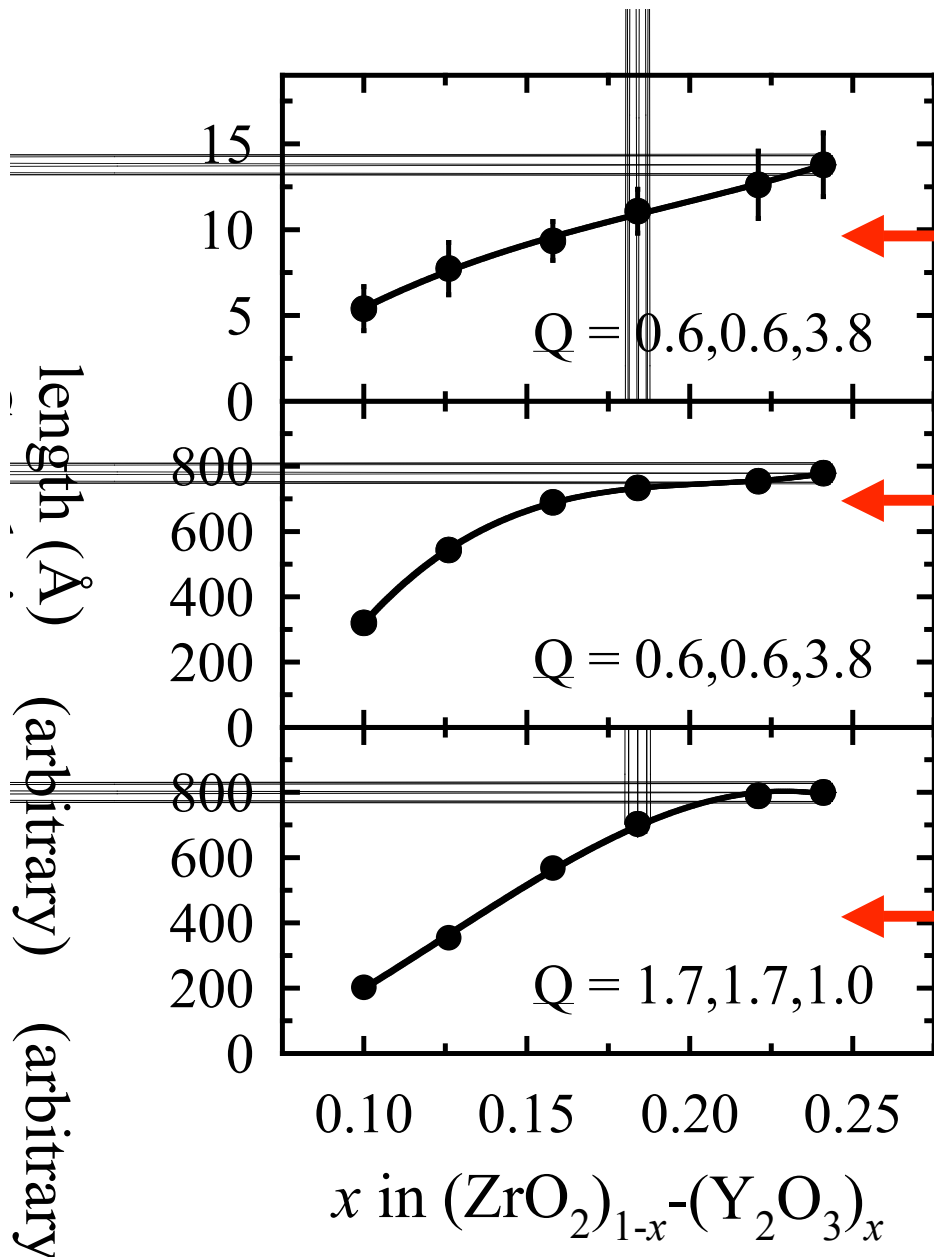


$x=0.126(5)$  sample.

The diffuse scattering arising from the presence of isolated O<sup>2-</sup> vacancies is strongly broadened in energy transfer, with a Lorentzian profile (convolved with the Gaussian instrument resolution function).

□ highly mobile isolated vacancies.

# ZrO<sub>2</sub>-Y<sub>2</sub>O<sub>3</sub> : CONCENTRATION DEPENDENCE



The width in  $Q$  of the  $q=0.4, 0.4, 0.8$  type peaks gives an indication of the aggregate size.

□ size increases with  $x$ .

The peak intensity is a measure of the defect concentration.

□ number increases initially with  $x$  and is then constant.

The intensity of the diffuse scattering at  $Q \sim 1.7, 1.7, 1.0$  indicates that the number of isolated  $\text{O}^{2\ominus}$  vacancies increases with  $x$  and then saturates.

# CONCLUSIONS

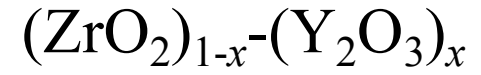
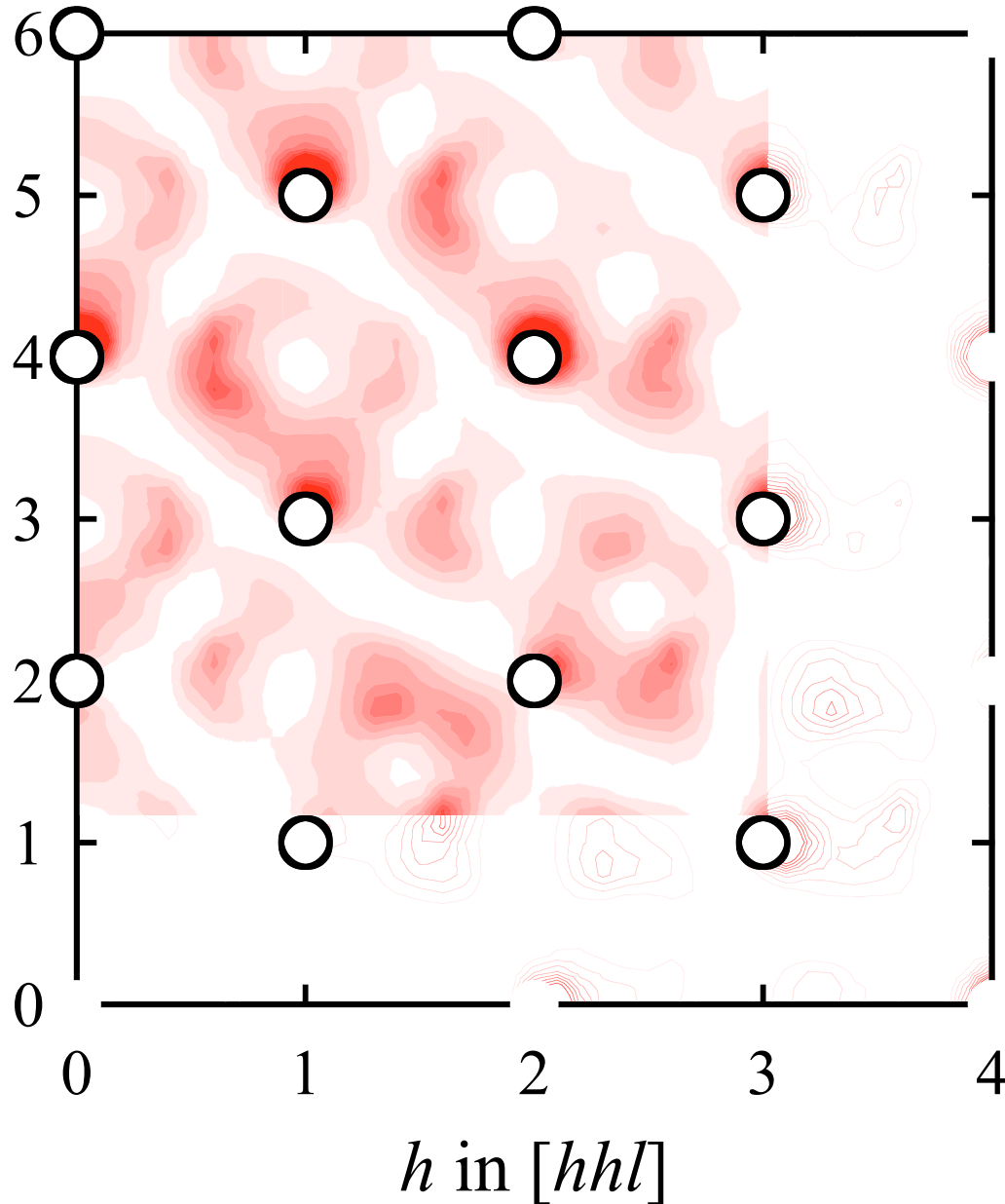
- Diffuse neutron scattering is a powerful technique to determine the structure of defects within ionic conductors, but don't ignore Bragg scattering!
- Simultaneous least-squares fitting of both Bragg and diffuse scattering data can be a valuable approach, especially at elevated temperatures where large thermal vibrations restrict the extent of high  $Q$  data.
- Quasielastic broadening of the diffuse scattering can probe the dynamics of the defects as a function of temperature and help explain the macroscopic behaviour of the ionic conductivity with temperature and/or dopant concentration.



# ZrO<sub>2</sub>-Y<sub>2</sub>O<sub>3</sub> : DIFFRACTION STUDIES

- 'The Structure of Cubic ZrO<sub>2</sub>:YO<sub>1.5</sub> Solid Solutions by Neutron Scattering', D.Steele and B.E.F.Fender, *J. Phys. C: Solid State Phys.*, **7**, 1 (1974).
- 'Neutron-Diffraction Study of Zr(Ca,Y)O<sub>2-x</sub> : Evidence of Differing Mechanisms for Internal and External Distortions', J.Faber Jr., M.H.Mueller and B.R.Cooper, *Phys. Rev. B*, **17**, 4884 (1978).
- 'X-ray Diffraction Study of Zr(Ca,Y)O<sub>2-x</sub>. I. The Average Structure', M.Morinaga, J.B.Cohen and J.Faber Jr., *Acta Cryst.*, **A35**, 789 (1979).
- 'X-ray Diffraction Study of Zr(Ca,Y)O<sub>2-x</sub>. II. Local Ionic Arrangements', M.Morinaga, J.B.Cohen and J.Faber Jr., *Acta Cryst.*, **A36**, 520 (1980).
- 'X-ray Diffraction Study of Zr(Ca,Y)O<sub>2-x</sub>; The Disordered State', J.B.Cohen, M.Morinaga and J.Faber Jr., *Solid State Ionics*, **3-4**, 61 (1981).
- 'Time-of-Flight Neutron Diffraction Study of a Single Crystal of Yttria-Stabilized Zirconia, Zr(Y)O<sub>1.862</sub>, at High Temperature and in an Applied Electrical Field', H.Horiuchi, A.J.Schultz, P.C.W.Leung and J.M.Williams, *Acta Cryst.*, **B40**, 367 (1984).
- 'Neutron Scattering Investigation of the Defect Structure of Y<sub>2</sub>O<sub>3</sub> - Stabilised ZrO<sub>2</sub> and its Dynamical Behaviour at High Temperatures', R.Osborn, N.H.Andersen, K.Clausen, M.A.Hackett, W.Hayes, M.T.Hutchings and J.E.MacDonald, *Mater. Sci. Forum*, **7**, 55 (1986).
- 'Structures of the ZrO<sub>2</sub> Polymorphs at Room Temperature by High Resolution Neutron Powder Diffraction', C.J.Howard, R.J.Hill and B.E.Reichert, *Acta Cryst.*, **B44**, 116 (1988).
- 'Defect Structure of Zirconia (Zr<sub>0.85</sub>Ca<sub>0.15</sub>O<sub>1.85</sub>) at 290 and 1550K', R.B.Neder, F.Frey and H.Schulz, *Acta Cryst.*, **A46**, 799 (1990).
- 'Diffuse Scattering in Yttria-Stabilized Cubic Zirconia', T.R.Welberry, R.L.Withers, J.G.Thompson and B.D.Butler, *J. Solid State Chem.*, **100**, 71 (1992).
- 'Defect Structure and Diffuse Scattering of Zirconia Single Crystals Doped with 7mol% CaO', T.Proffen, R.B.Neder, F.Frey and W.Assmus, *Acta Cryst.*, **B49**, 599 (1993).
- 'A 3D Model for the Diffuse Scattering in Cubic Stabilized Zirconias', T.R.Welberry, B.D.Butler, J.G.Thompson and R.L.Withers, *J. Solid State Chem.*, **106**, 461 (1993).
- 'Defect Structure and Diffuse Scattering of Zirconia Single Crystals with 10 and 15mol% CaO at Temperatures up to 1750K', T.Proffen, R.B.Neder, F.Frey, D.A.Keen and C.M.E.Zeyen, *Acta Cryst.*, **B49**, 605 (1993).
- 'Measurement of the Static Disorder Contribution to the Temperature Factor in Cubic Stabilized ZrO<sub>2</sub>', D.N.Argyriou, *J. Appl. Cryst.*, **27**, 155 (1994).
- 'Re-Investigation of Yttria-Tetragonal Zirconia Polycrystal (Y-TZP) by Neutron Powder Diffraction - A Cautionary Tale', D.N.Argyriou and C.J.Howard, *J. Appl. Cryst.*, **28**, 206 (1995).
- 'Oxide Ion Transport in Highly Defective Cubic Stabilized Zirconias', J.T.S.Irvine, I.R.Gibson and D.P.Fagg, *Ionics*, **1**, 279 (1995).
- 'Neutron and X-ray Diffuse Scattering of Calcium-Stabilized Zirconia', T.Proffen, R.B.Neder and F.Frey, *Acta Cryst.*, **B52**, 59 (1996).
- 'Neutron and X-ray Diffuse Scattering of Calcium-Stabilized Zirconia at Temperatures up to 1500K', T.Proffen, M.Keilholz, R.B.Neder, F.Frey and D.A.Keen, *Acta Cryst.*, **B52**, 66 (1996).
- 'A Neutron Scattering Investigation of Cubic Stabilised Zirconia (CSZ) - I. The Average Structure of Y-CSZ', D.M.Argyriou, M.M.Elcombe and A.C.Larson, *J. Phys. Chem. Solids*, **57**, 183 (1996).
- 'Study of the Order-Disorder Transition in Yttria-Stabilised Zirconia by Neutron Diffraction', I.R.Gibson and J.T.S.Irvine, *J. Mater. Chem.*, **6**, 895 (1996).
- 'Analysis of the Diffuse Neutron and X-ray Scattering of Stabilised Zirconia Using the Reverse-Monte-Carlo Method', T.Proffen, *Physica B*, **241-243**, 281 (1998).
- 'Defect Structure of Yttria-Stabilized Zirconia and its Influence on the Ionic Conductivity at Elevated Temperatures', J.P.Goff, W.Hayes, S.Hull, M.T.Hutchings and K.N.Clausen, *Phys. Rev. B*, **59**, 14202 (1999).

# ZrO<sub>2</sub>-Y<sub>2</sub>O<sub>3</sub> : DIFFUSE SCATTERING



$$x=0.184(7)$$

Calculated diffuse X-ray scattering using the proposed defect model is in good agreement with measured data.